~~CONFIDENTIAL RESTRICTED DATA~~

NPO-0

RECORD COPY

REON

SACRAMENTO PLANT

RN-S-0217

MASTER

A Report To

AEC-NASA SPACE PROPULSION OFFICE

FINAL REPORT FOR PHASE I-B OF THE COUNTERMEASURES RADIATION EFFECTS PROGRAM (U)

Contract SNP-1 April 1965 NERVA Program

~~RESTRICTED DATA ATOMIC ENERGY ACT 1954~~

AEROJET GENERAL TIRE GENERAL

DISCLAIMER

[redacted] RESTRICTED DATA

AEROJET GENERAL

Classification cancelled (~~or changed to~~)
by authority of DOE
by W. C. TIC, date SEP 10 1973

RN-S-0217

A Report To

AEC-NASA SPACE PROPULSION OFFICE

FINAL REPORT FOR PHASE I-B OF THE COUNTERMEASURES RADIATION EFFECTS PROGRAM (U)

SPECIAL REREVIEW FINAL DETERMINATION	Reviewers	Class.	Date
Class: U	JRP	U	02/25/82
	LNR	U	03/16/82

ROCKET ENGINE OPERATIONS – NUCLEAR

Contract SNP-1 April 1965 NERVA Program

[redacted]

GROUP 1

~~Excluded from Automatic Downgrading and Declassification~~

AEROJET-GENERAL CORPORATION
A SUBSIDIARY OF THE GENERAL TIRE & RUBBER COMPANY

DISTRIBUTION OF THIS DOCUMENT UNLIMITED

MASTER

[redacted]

RN-S-0217

FOREWORD

Presented within this document are the test results of Phase I-B of the Countermeasure Radiation Effects Program, Sub-Subtask 1.9.1, which evolved from the combined efforts of Aerojet-General REON and Ordnance Research Divisions, the General Electric Company Vallecitos Atomic Laboratory, and the United States Army Picatinny Arsenal Ammunition Engineering Directorate and Explosives Research Laboratory.

This document is submitted in partial fulfillment of Contract SNP-1, Subtask 1.9.

W. D. Stinnett
Program Manager
Rocket Engine Operations - Nuclear

CONTENTS

CONTENTS (cont.)

CONTENTS (cont.)

I. INTRODUCTION

This phase of the Countermeasures Radiation Effects Program, REON Sub-subtask 1.9.1, was concerned with evaluation of high-temperature-stable explosives and propellants. Results of Phase I indicated that high-temperature stability and the presence of an aromatic structure imparted radiation stability to explosive compounds, and that composite propellants were radiation-stable. Therefore, this phase investigated the best materials from Phase I (DATB explosive and ANP 3095 propellant), other aromatic high-temperature-stable explosives (TATB, DIPAM, HNS, and NONA), high-temperature-stable propellant AK-14, black powder, and two special high-temperature explosives obtained by NASA. High-temperature stability is necessary because of the high gamma heating rate, and is particularly important for an uncooled destruct system on the NERVA II engine.

This program was performed under the joint direction of Aerojet-General Corporation (REON Division), U.S. Army Picatinny Arsenal, and General Electric Company Irradiation Processing Operations. Samples were irradiated in the GE Test Reactor at Vallecitos, Calif. Subsequent tests on irradiated samples were performed jointly by Aerojet-General's Downey Ordnance Research Division and U.S. Army Picatinny Arsenal personnel in the GE Radiological Materials Laboratory. Test procedures and a description of materials tested have been reported in "Addendum No. 2 to Report 2510, Final Test Specifications for Phase I-B of the Countermeasures Radiation Effects Program, published by Aerojet-General Corporation (REON Division), Sept 1964.

A complete compilation of data and summary of results has been reported by GE in their "Countermeasures Radiation Effects Program Phase I-B Data Summary and Final Report" (Reference 1). The present report by Aerojet-General personnel presents the conclusions that can be made based on this data.

II. SUMMARY

The materials tested in Phase I-B are listed in Table 1 in order of their relative radiation stability (based on weight loss). All samples were evaluated after exposure to the integrated dose produced by a 120-min exposure; therefore, only the data from this exposure are shown for comparison purposes. A complete summary of the data is presented in the GE Final Report for Phase I-B (Reference 1). The best materials survived 180-min exposure to the peak GETR flux which produced total combined integrated doses of 1.2×10^9R gamma, 1.4×10^{17} n/cm^2 fast neutrons (> 0.18 mev), 2×10^{17} n/cm^2 intermediate neutrons (0.17 ev $\longrightarrow$ 0.18 mev), and 9.2×10^{17} n/cm^2 thermal neutrons (< 0.17 ev).

Because of the high rate of gamma heating and the difficulty in cooling a destruct system, high-temperature stability combined with radiation stability will be required. This is particularly true of the main charge explosive, since it will be exposed to the highest heating rate as shown in Figure 1. Differential thermal analysis (DTA), vacuum stability, and explosion temperature were used to measure thermal stability. Of these methods, the DTA most closely approximates the heating rate expected in the destruct system, and is therefore of the greatest importance in the selection of high-temperature materials. The relative thermal stability shown in Table 1 (based on DTA results) indicates that NASA-1 or TATB are the most resistant explosives. However, when both heating and radiation are taken into account, DATB is expected to be the best explosive. This is because the larger amount of decomposition of the other materials during radiation would add to their rate of temperature rise, while melting of DATB would decrease its heating rate. The other explosives should also be tested further as a back-up in the event that melting of DATB above 282°C cannot be tolerated.

Two booster explosives were considered: NONA and HNS. There were certain advantages in the use of NONA (higher thermal stability and lower weight loss) but these gains were more than offset by higher cost and greater procurement problems. For the base fuzing system shown in Figure 1, the temperature stability of HNS should be entirely adequate. Thus, HNS will be used in preference to NONA.

On the basis of weight loss alone, the ANP 3095 propellant was slightly better than AK-14. But where high temperature stability is required, AK-14

TABLE 1

SUMMARY OF EFFECTS OF NUCLEAR RADIATION
(AFTER 120 MIN EXPOSURE* AT PEAK FLUX)

Use	No.	Material	Wt Loss %	DTA Exotherm Peak (°C)**		5 sec Explosion Temp, °C		% Change		Order of Stability	
				Standard	Irrad	Standard	Irrad	Expl Temp (5 sec)	DTA Exotherm**	Temp	Wt
Main Charge	W	DATB	0.59	358	355	403	344	-14.6	0.8	3	1
	H	TATB	0.79	388	365	392	287	-26.8	5.9	2	2
	A	NASA-1	0.84	398	388	417	374	-10.3	2.5	1	3
Main Charge	O	DIPAM	2.0	312	265	371	287	-22.6	13.1	4	4
Booster	J	NONA	1.79	402	365	440	360	-18.2	9.2	1	1
Booster	V	HNS	2.44	353	330	382	314	-17.8	6.4	2	2
Propellant	R	ANP 3095	6.26	260	285	317	159	-49.8	-9.6	2	1
Propellant	E	AK-14	8.0	485	468	406	319	-21.4	3.5	1	2
Initiator	S	Black Powder	0.21	327	324	324	298	- 8.0	0.9		
Primary	L	NASA-2	23.6	380	315	375	224	-40.3	17.1		

*The following exposures were involved:
Gamma: 4×10^8 R/hr, 8×10^8 R
Fast Neutrons (>0.18 mev): 1.3×10^{13} n/cm^2/sec, 9.4×10^{16} n/cm^2
Intermediate Neutrons (0.17 ev → 0.18 mev): 1.8×10^{13} n/cm^2/sec, 1.3×10^{17} n/cm^2
Thermal Neutrons (< 0.17 ev): 8.5×10^{13} n/cm^2/sec, 6.1×10^{17} n/cm^2

**Heating rate of 20°C/min

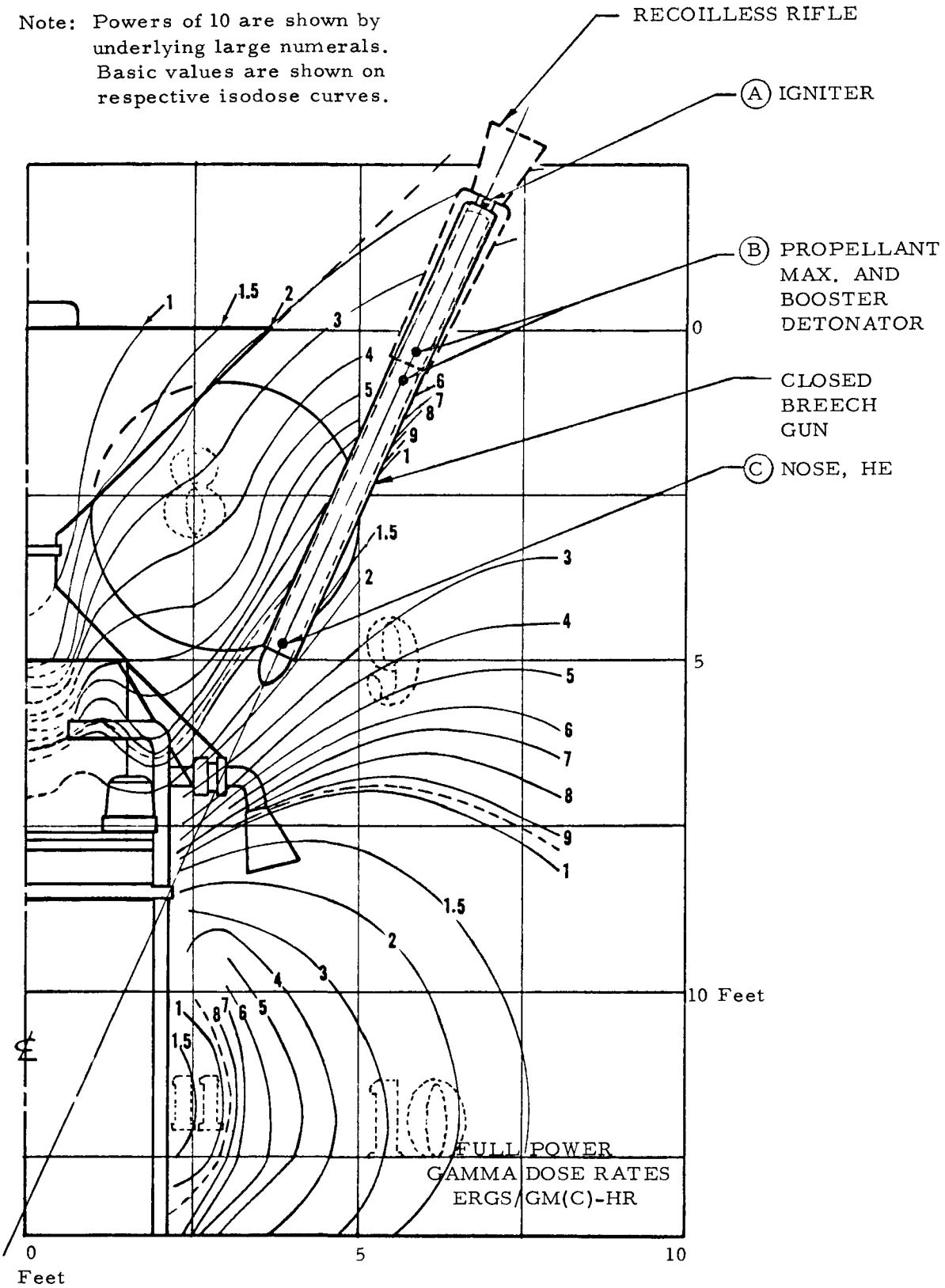

Figure 1

NERVA Gamma Dose Rates on Destruct System Components

should be used in preference to ANP 3095 since its temperature tolerance level is 200°C higher (i.e., up to 468°C). Unfortunately, this increase in temperature stability is purchased at the cost of a reduction in performance from a force of 355,000 to 180,000 ft-lb/lb. Therefore, a composite propellant such as ANP 3095, which has ammonium perchlorate, should be used in systems where lower temperature stability is permissible. (Such a system is shown in Figure 2 where the propellant is exposed to about one-fifth the flux the explosive receives.) Additional testing of the higher-temperature-stable potassium perchlorate oxidized propellants should continue as a back-up (Appendix B).

Because of its high radiation resistance (over 10^9 R gamma) and high temperature stability (about 300°C), black powder is not expected to cause any igniter design restrictions in the location at the rear of the projectile shown in Figure 2. Of the explosives tested, black powder was the most radiation-stable (based upon weight loss). Its high degree of radiation stability was due to the absence of organic materials which are easily damaged by radiation.

It may be possible to fabricate a radiation-stable exploding bridgewire detonator without the use of a primary explosive (Reference 2). However, as a back-up, NASA supplied a very high-temperature stable (to 368°C) primary explosive which was designated NASA-2. This explosive was tested in this phase. This material did not have a benzenoid resonance, and was damaged to a greater extent than any of the other materials.

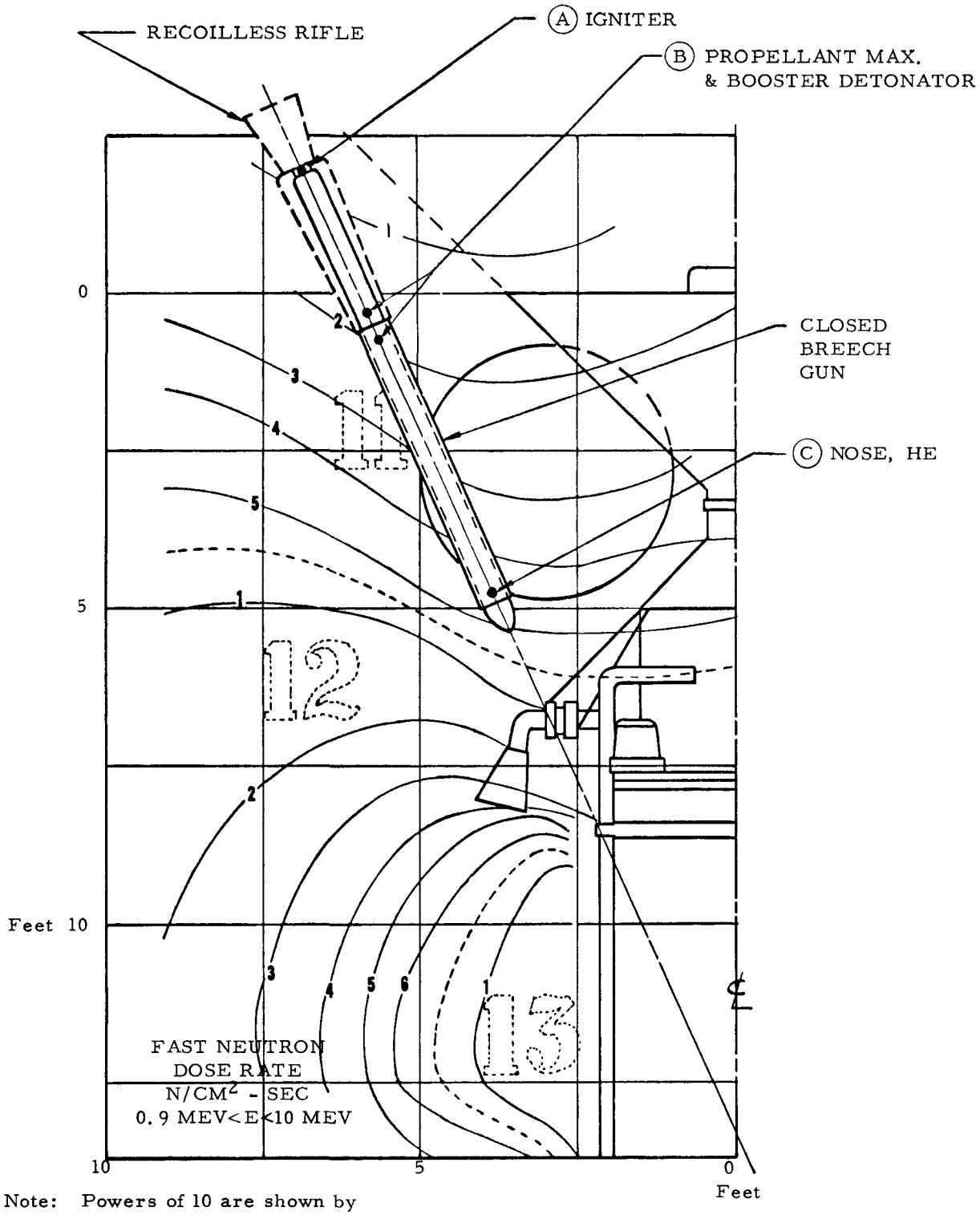

Note: Powers of 10 are shown by underlying large numerals. Basic values are shown on respective isodose curves.

Figure 2

NERVA Neutron Flux Rates on Destruct System Components

III. TECHNICAL DISCUSSION

A. RADIATION ENVIRONMENT

Figures 1 and 2 illustrate expected positioning of the Countermeasure projectile on a NERVA I engine. The components of the projectile of particular interest are designated at positions A, B, and C. For example, position A designates the location of the propellant igniter - the component which would experience the least amount of radiation on a total system comparison. Position B represents the location of the propellant, primary (initiating), and booster type materials, while position C represents the main charge location and area of maximum radiation.

Table 2 compares the various neutron fluxes and gamma dosages of these materials in their respective locations with the radiation environment available at the General Electric Test Reactor. Also, a comparison of 20-, 40-, and 60-min runs of both a NERVA I and NERVA II (Phoebus) engine are provided to illustrate the various total integrated fluxes and dosages. The NERVA I flux data was extrapolated from an October 1964 NERVA isoflux map, while the NERVA II flux data was based on estimated factors of 2.7 for fast neutrons and 5.0 for gammas. It should be pointed out that projectile relocation, shield modification, or reactor changes will substantially change these radiation values. In fact, Table 2 is included here primarily to demonstrate the need for determining the radiation tolerance of many of these components.

Based on the dose rates provided in Table 2, possible heating rates of these materials have been calculated using the method described in Appendix C of Aerojet Report RN-S-0210.* NERVA II heating rates are as follows:

3.2°C/min for position A
7.7°C/min for position B
22.2°C/min for position C

It appears the temperature stability of the main charge explosive in position C will be a critical design factor unless some form of cooling or shielding is provided.

*Final Test Report for Phase One of the Countermeasure Radiation Effects Program, Aerojet Report RN-S-0210, April 1965.

TABLE 2

RADIATION FLUXES AND DOSAGES*

Gamma Radiation

Component	Location	Dose Rate 10^9 ergs/g(C)/hr				Integrated Dose 10^9 ergs/g(C)												
		NERVA I	NERVA II	GETR		NERVA I			NERVA II			GETR Max			GETR Reduced			
		Max	Max	Max	Reduced	20 min	40 min	60 min	20 min	40 min	60 min	9 min	25 min	125 min	9 min	25 min	75 min	125 min
Igniter	A	0.4	3.0	-	-	0.13	0.27	0.4	1.0	2.0	3.0	-	-	-	-	-	-	-
Propellant, Max Primary Explosive Booster Explosive	B	1.0	7.5	36.8	9.65	0.33	0.67	1.0	2.5	5.0	7.5	5.34	15.35	76.5	1.40	4.03	12.08	-
Main Charge Explosive	C	3.0	22.5	36.8	9.65	1.0	2.0	3.0	7.5	15.0	22.5	5.34	15.35	76.5	-	-	-	20.1

Fast Neutron Radiation (0.9 mev → 10 mev)

Component	Location	Flux Rate 10^{12} n/cm^2-sec				Integrated Flux 10^{15} n/cm^2												
		NERVA I	NERVA II	GETR		NERVA I			NERVA II			GETR Max			GETR Reduced			
		Max	Max	Max	Reduced	20 min	40 min	60 min	20 min	40 min	60 min	9 min	25 min	125 min	9 min	25 min	75 min	125 min
Igniter	A	0.2	0.81	-	-	0.24	0.48	0.72	0.96	1.95	2.91	-	-	-	-	-	-	-
Propellant, Max Primary Explosive Booster Explosive	B	0.4	1.62	7.1	1.2	0.48	0.96	1.44	1.95	3.90	5.82	3.8 ~~7.36~~	10.1 ~~21.15~~	56 ~~105.75~~	0.65 ~~1.25~~	1.8 ~~3.6~~	5.4 ~~10.8~~	-
Main Charge Explosive	C	1.0	4.05	7.1	1.2	1.20	2.40	3.60	4.86	9.72	14.58	3.8 ~~7.36~~	10.1 ~~21.15~~	56 ~~105.75~~	-	-	-	-

*Based on isoflux map of the NERVA engine dated October 1964. NERVA II fluxes are assumed to be 2.7 times the NERVA I neutron flux and 5 times the NERVA I gamma dose rate.

B. WEIGHT LOSS

Weight loss continued to be an important measure of radiation damage. With this measurement, changes in density, detonation velocity, and total blast effect, can be predicted, and the amount of gas released calculated. The most stable material in Phase I-B was black powder - an inorganic mixture. This material plus four main charge explosives (DATB, NASA-1, TATB and DIPAM) and the HNS booster explosive survived a 3-hour exposure of 10^{11} erg/g (C) integrated gamma dose and an integrated fast neutron flux of 1.5×10^{17} nvt ($E > 0.18$ mev) without loosing more than 5% of their weight. Because of excessive decomposition at lower dosages, all materials were not exposed for 3 hours; however, comparative data was obtained at an integrated gamma dose of 6.8×10^{10} erg/g (C), plus an integrated fast neutron flux of 9.4×10^{16} nvt ($E > 0.18$ mev). The materials tested are listed in order of stability in Table 3, with each material's tolerance value extrapolated from the weight loss data provided in Figures 3 and 4.

A summary of all weight loss data is given in Table 4. Where measured weight loss was not obtained, or was grossly in error, a weight loss calculated from the amount of gas released is reported. The method of making this calculation is described in Section III,C. Errors in weight loss occurred when the quartz vials were chipped during unloading, and when damaged fragments of the pressed pellets fell out of the detonation velocity tubes.

Samples were weighed and witnessed at the time of loading, using an analytical balance accurate to ± 0.0002 g and checked against standard weights. After removal from the capsules, the sample tubes were weighed on a similar balance checked against the same standard weights. Although weighing errors were improbable, one obvious error occurs on the AGO-4 sample where weight apparently increased. The error is believed to be due to faulty data recording, since balance readings were double checked. On the other hand, high weight losses may have been caused by the way the samples were handled due to their radioactivity. Volatile liquids such as water, methanol, and formaldehyde may have been partially lost due to evaporation between the time the capsules were opened and the samples weighed, or weight gained due to the adsorption of moisture prior to weighing.

TABLE 3

MAXIMUM INTEGRATED FLUX AND DOSE VALUES*

Type	Material	Code	Gamma R x 10^{-8}	Fast Neutrons, E > 0.18 mev (n/cm^2 x 10^{-16})	Intermediate Neutrons, 0.17 ev-0.18 mev (n/cm^2 x 10^{17})	Thermal Neutrons (n/cm^2 x 10^{-17})
Main charge explosive	DATB	AGW	16.8	19.08	2.80	14.43
	TATB	AGH	18.0	21.02	3.26	14.93
	NASA-1	AGA	16.5	18.88	2.77	13.36
	DIPAM	AGO	12.0	12.77	1.87	8.88
Booster explosive	NONA	AGJ	13.4	15.12	2.25	10.70
Booster explosive	HNS	AGV	11.2	13.57	2.02	9.18
Primary explosive	NASA-2	AGL	0.2	0.26	0.04	0.169
Initiator	Black powder	AGS	>7.8	>8.40	>1.20	>6.10
Composite propellant	ANP 3095	AGR	7.4	8.42	1.22	6.19
Composite propellant	AK-14	AGE	7.6	8.33	1.24	5.85

* For approximately 5% weight loss.

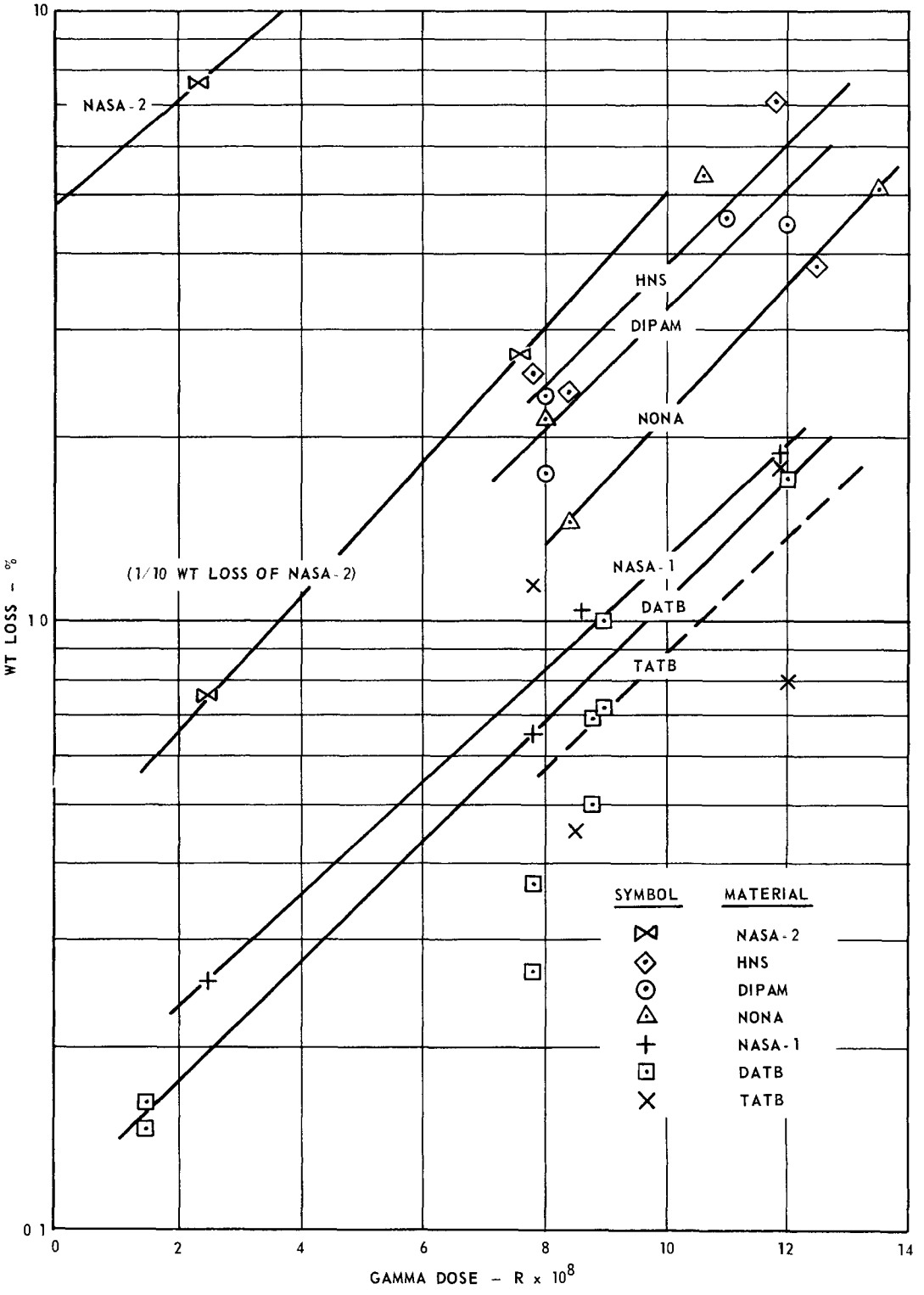

Figure 3

Weight Losses of Explosives

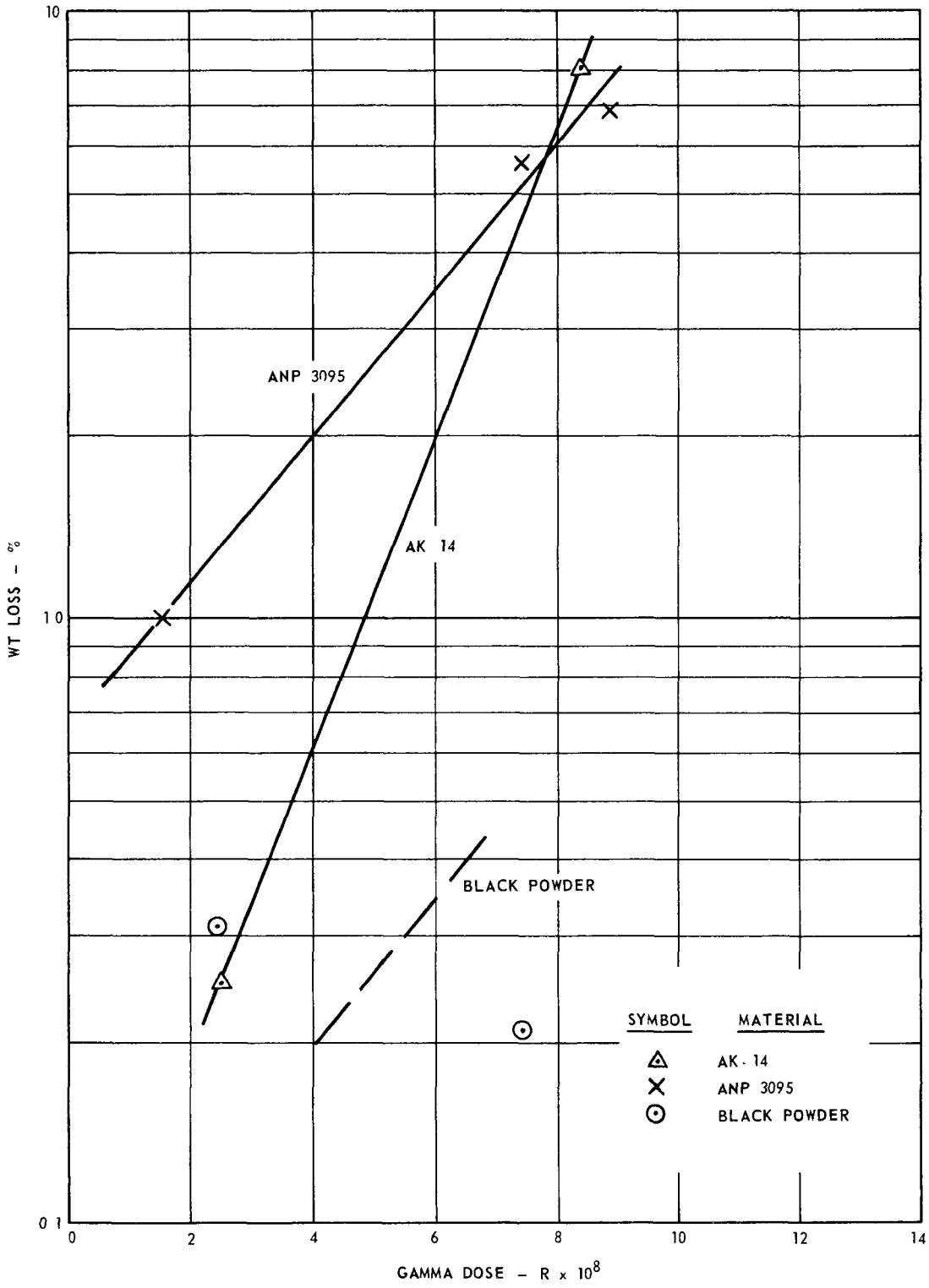

Figure 4

Weight Losses of Propellants

TABLE 4

WEIGHT LOSS SUMMARY

Sample No.	Material	Weight Loss (%) at Indicated Exposure Times 36 min	120 min	180 min	Remarks
A	NASA-1	0.257	1.03	1.87	Main charge
A	NASA-1	-	0.65	-	
E	AK-14	0.25	8.05	-	Propellant
F	DIPAM	2.50	8.82	-	MDF same as O (data not accurate because of small amount measured)
H	TATB	-	0.45	0.79	Main charge
H	TATB	-	1.14	1.79*	
J	NONA	-	1.45*	5.09	Booster
J	NONA	-	2.14*	5.31*	
L	NASA-2	7.52	23.6	-	Least stable (only primary explosive tested)
M	DATB	0.565	2.73	-	MDF same as W
M	DATB	0.521	2.88	-	
O	DIPAM	-	2.34	4.44	Least stable of main charge explosives
O	DIPAM	-	1.73*	4.55*	
R	ANP 3095	-	5.64	-	Propellant
R (Phase I)	ANP 3095	1.0	6.89	-	Propellant
S	Black Powder	0.31	0.21	-	Initiator
V	HNS	-	2.36	3.80*	Booster
V	HNS	-	2.52	7.02*	
W	DATB	-	0.26	1.70*	Lowest weight loss(main charge)
W	DATB	-	0.37*	-	
W (Phase I)	DATB	0.162	0.69	-	
W (Phase I)	DATB	0.146	0.50	-	
W (Phase I)	DATB	-	0.71	-	
W (Phase I)	DATB	-	1.00	-	
T	NASA-1	-	2.03	4.29*	Lead melted on one end of 180 min. samples (MDF form)

Integrated Exposure:

Total gamma dosage, ergs/g (C) x 10^{-10}: 2.5 (at 36 min), 7.1 (at 120), 10.7 (at 180 min)
Fast neutrons ($>$ 0.18 mev), nvt x 10^{-16}: 2.77 (at 36 min) 9.42 (at 120 min) 14.52 (at 180 min)
Thermal neutrons ($<$ 0.18 mev), nvt x 10^{-17}: 1.98 (at 36 min), 6.54 (at 120 min), 10.38 (at 180 min)

*Calculated from gas volume

Table 4

Black powder (AGS) - a mixture of inorganic materials - showed the lowest weight loss. The main charge explosives (DATB (AGW), NASA-1 (AGA), and TATB (AGH) were also very stable, and all lost (or would have lost) less than 2 wt%, even after 180 min of exposure to the peak flux. The HNS (AGV) booster explosive lost approximately 5 wt% at this flux.

The weight loss of explosives in MDF form was higher than in powder form. This is believed to be due to increased gamma heating and decreased cooling. For example, the temperature of the AGT sample was high enough (approximately 300°C) to slightly melt the end of the lead sheath.

The only primary explosive tested, NASA-2 (AGL), experienced the least radiation stability, even though its temperature-stable limit exceeded 300°C. Since lead azide has a similar chemical composition, and also has low radiation stability (References 3 and 4), a benzoid structure appears mandatory for this program.

Irradiations were performed under approximately isothermal conditions at a temperature of 90°C. Weight loss vs integrated gamma dosage is plotted in Figures 3 and 4 to permit extrapolation to different dosages. These figures indicate the decomposition is approximately a first-order decomposition relationship (Reference 5), as observed by Kaufman (Reference 6) for explosives exposed to pure gamma irradiation. Additional data will be obtained in subsequent phases when a continuous measurement is made of gas released during irradiation.

C. RADIOLYTIC GAS RELEASE

Radiolytic gas volume was determined by measuring the pressure, temperature, and internal volume in the capsules subsequent to irradiation using the system illustrated in Figure 5. These results and measurements are provided in Table 5. This data was also used to calculate the gas volume at standard conditions. The gas volume measurements are considered accurate to within ±0.5 cu cm except on capsules where leaks occurred in the perforating system. These leaks occurred when aluminum chips from the drill penetrated the O-ring seals of the perforating head. Unfortunately, by the time they were detected, some gas had already escaped.

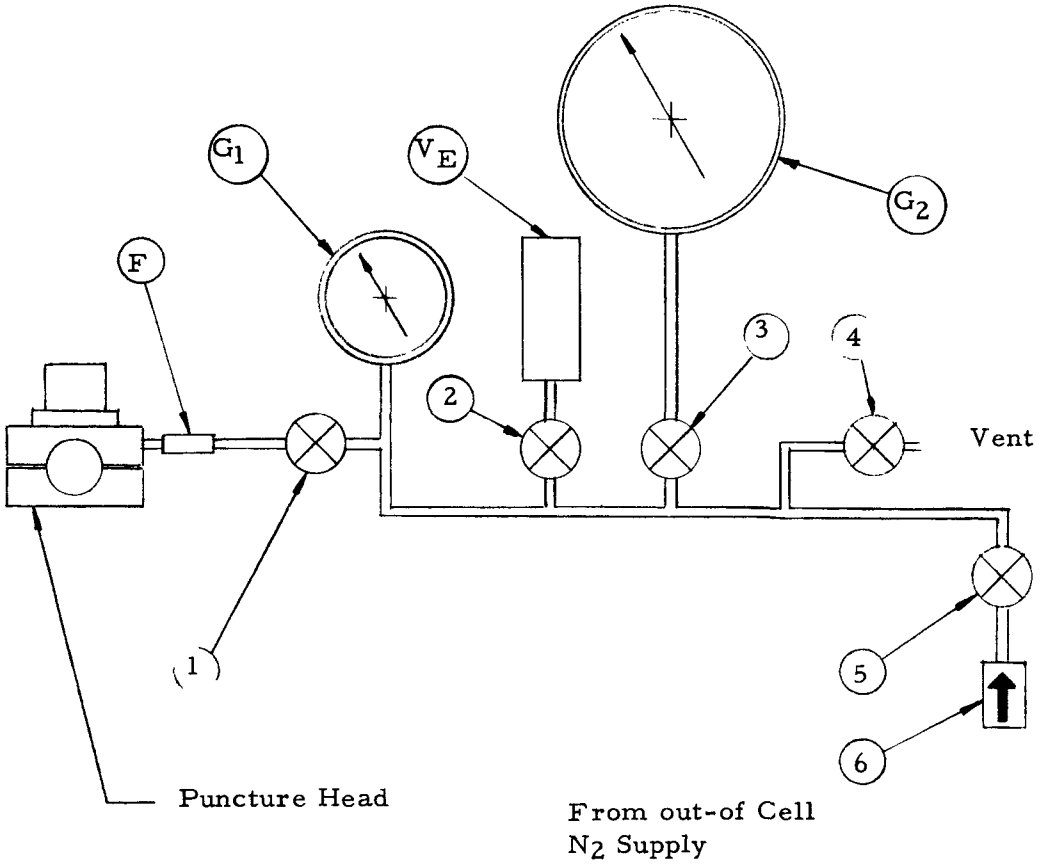

No.	Req'd	Description
1	1 ea	Valve, 1/4" size, stainless steel
2	1 ea	" " " " "
3	1 ea	Valve, 1/4" size, stainless steel
4	1 ea	" " " " "
5	1 ea	Valve, 1/4" size, stainless steel
6	1 ea	Check Valve
G_1	1 ea	Pressure Gage; 0-100 psig, stainless steel
G_2	1 ea	Pressure Gage; 0-15 psig, stainless steel, graduations at 2mm Hg intervals, 0.2% of full scale accuracy; Wallace & Tiernan FA 145
V_E	1 ea	Expansion Tank; stainless steel, Volume 159.5 cc
F	1 ea	Filter, Stainless Steel

Figure 5

Radiolytic Gas Measurement Apparatus

TABLE 5

RADIOLYTIC GAS RELEASE SUMMARY

		Loading Conditions		Post-Irradiation				Calculated Values			
Sample No.	Material	Temperature (°F)	Pressure (mm Hg)	Weight Loss (g)	Pressure (mm Hg)	Temperature (°F)	Void Vol (cu cm)	Gas Vol (cu cm at STP)	Gas Vol (cu cm/g sample)	Radiolytic Gas (cu cm/g decomposed)	Equivalent wt Explosive Loss (g)
A-1	NASA-1	74	760.5	0.0047	771.7	72	46.6	0.855	0.47	182	0.0012
A-2		81	760.5	0.0181	945.2	82	48.3	11.349	6.46	627	0.0170
A-3		72	757.7	0.0326	1131.07	80	49.8	23.185	13.28	711(1)	0.0326
A-4		72	757.7	0.0117	981.0	80	49.4	13.193	7.35	1127	0.0185
T-1		74	761.3	0.0062	755.9	72	50.5	0	0	-	-
T-2	NASA-1	78	761.3	0.0247	899.6	72	48.4	9.29	30.10	384	0.0131
E-1	AK-14	69	759.7	0.0045	830.0	80	46.6	3.267	1.84	726(1)	0.0045
E-2	AK-14	67	759.7	0.1466	2262.7	80	-	36.206	19.88	243	0.0498
H-1	TATB	85	759.5	0.0144	813.8	80	48.1	3.789	2.06	263(5)	0.00485
H-2		85	759.5	0.0083	751.2	80	50.4	0	0	- (5)	-
H-3		74	757.7	0.1540(3)	1160.7	80	49.6	25.187	14.01	164(3)	0.0322
H-4	TATB	74	757.7	0.0197	798.7	80	48.2	2.016	1.16	102	0.0026
J-1	NONA	74	756.2	0.0895	1636.2	79	48.4	54.456	30.92	608	0.0681
J-2		74	756.2	0.1449(3)	1092.4	80	47.9	20.196	11.54	139(3)	0.0254
J-3		74	758.5	0.1664(3)	1902.7	80	49.2	71.959	42.10	431(3)	0.0906
J-4	NONA	74	758.5	0.0530	1225.6	82	50.3	29.386	17.00	554	0.0370
L-2	NASA-2	78	754.9	0.422	3396.2	80	48.7	165.315	92.30	382	0.2035
L-3	NASA-2	65	757.4	0.1391	2532.2	80	50.3	113.457	61.50	814(1)	0.1391
O-1	DIPAM	70	761.5	0.0805	1602.5	80	49.3	48.177	26.55	597	0.0481
O-2		70	761.5	0.0421	1147.6	80	46.8	22.382	12.40	525	0.0283
O-3		74	757.7	0.1148	1795.0	80	49.3	65.25	35.95	568	0.0826
O-4		74	757.7	- (4)	1154.0	80	50.8	25.329	13.70	- (4)	0.0320
F-1		65	757.4	0.0027	767.4	80	50.4	0	0	-	-
F-2	DIPAM	65	757.4	0.0102	795.5	80	49.8	1.052	9.11	103	0.0013
R-2	ANP 3095	74	759.7	0.1030	1864.6	81	50.2	70.515	38.61	685	0.0871
S-1	Black Powder	75	754.9	0.0056	766.0	80	46.6	0.243	0.13	434(1)	0.0056
S-2	Black Powder	75	754.9	0.0038	755.3	80	48.2	0	0	-	-
V-1	HNS	71	759.5	0.2652(3)	1600.7	82	50.1	53.052	29.80	200(3,5)	0.0076
V-2		80	760.5	0.0413	1182.1	78	47.2	25.869	14.76	627	0.0327
V-3		66	757.7	0.1706	2304.8	80	49.4	96.965	55.80	570	0.1220
V-4	HNS	66	757.7	0.0432	1327.7	80	48.4	34.237	20.00	793(1)	0.0432
W-1	DATB	74	758.5	0.0048	857.1	80	48.9	5.663	3.12	118	0.0072
W-3		74	758.5	0.0470	1131.8	72	48.7	23.928	13.31	509	0.0305
W-4		75	757.7	0.0248	843.0	81	50.7	4.998	2.92	201	0.0064
M-1		80	756.9	0.0036	813.2	80	44.9	3.25	4.91	904	0.0041
M-2	DATB	80	756.9	0.0186	978.9	80	47.0	13.429	20.29	722	0.0171

(1) Used to calculate equivalent explosive weight.
(2) Assume gas composition is the same as that from explosion, and that all products formed from decomposition are gases, except for AGL.
(3) Weight loss was high due to handling losses (e.g., chipped tube, cracked pellet).
(4) Error in weighing resulted in negative weight loss.
(5) Leak in perforating system caused loss of gas.

The ratio of radiolytic gas (cu cm) to explosive lost (g) was used to calculate equivalent weight loss from gas volume measurements. Calculated values of this ratio are provided in Table 5. For samples where a reasonable ratio was obtained, this value was used to calculate equivalent weight loss. In cases where the observed ratios were inaccurate, the gas volume produced by explosion (Table 6) was used to calculate equivalent weight loss. (Gas volume values determined in this manner tend to be low since solid products of decomposition were not deducted from the weight of material decomposed.)

Table 6 provides a summary of gas volumes produced by decomposition of samples in the absence of air, with the volumes used for radiolytic gas release included for comparison. The average gas molecular weight was calculated from the gas volume per gram of gas.

Table 6 shows that observed and calculated volumes agree quite well in the cases where gas from explosion and radiolytic gas data are available, and where large amounts of solid residue are not produced. For NASA-2 and black powder, where large amounts of solid residue are found, theoretical gas molecular weights of 28.0 and 50.3, are used and then reasonable agreement is observed.

Gas generation was apparently uniform throughout the samples; consequently some of the gases produced were trapped inside the crystals of explosive, reducing the gas volume measured. Finely divided and loosely packed powders were used to minimize this effect. Since errors from this source are only a small percentage of the total error, calculated weight losses obtained from gas volumes were in reasonably close agreement with those observed. Therefore, it seems proper to use weight losses calculated from measured gas volumes in cases where accurate measured weight losses are not available.

D. DETONATION VELOCITY

Detonation velocity tests were performed on pressed explosive pellets and mild detonating fuzes. In general, detonation velocities decreased as a result of exposure to radiation. Within the accuracy of the test methods

TABLE 6

RELATIVE GAS VOLUMES

Material	Sample No.	Gas Released from Explosion (cu cm/g explosive)	Used in Calculations of Radiolylic Gas Release (cu cm/g gas)	Avg Gas Mol Wt
NASA-1	AGA	691	711	31.5
AK 14	AGE	723	726	30.8
TATB	AGH	781*	781	28.7
NONA	AGJ	794*	794	28.2
NASA-2	AGL	320	814	27.6
DIPAM	AGO	790*	790	28.4
Black powder	AGS	271	434	51.6
HNS	AGV	746	793	28.2
DATB	AGW	784*	784	28.6
ANP 3095	AGR	810*	810	27.7

*Used to calculate weight loss.

(±10%), this can be accounted for by the decrease in density caused by conversion of explosive molecules into gas. Velocity measurements were more accurate on MDF samples, than on explosive pellets. To offset this, pellet testing offered the following advantages:

1. Explosives not available in MDF form could be evaluated
2. Testing could be done after a shorter time lapse following irradiation
3. Density determinations were easier to make
4. The changes measured were more representative of those occurring in large explosive charges.

Detonation velocity and plate-dent were the only explosive performance tests made. The purpose of these tests was to determine the gross effect of nuclear radiation on explosive performance, and to use this information to select promising materials for further evaluation.

Radiation damage could affect detonation velocity in two ways: (1) by changing the chemical composition of the material being tested (solid decomposition products), and (2) by removing the explosive through conversion to gas (resulting in loss of density). The change in density was calculated from the decrease in weight and increase in length. (Increase in volume was assumed to be equal to the cube of the increase in length.)

1. Mild Detonation Fuze Test Method

The MDF samples were lead sheaths which confined the explosives in accordance with the loading characteristics of Table 7. Figure 6 illustrates the test fixtures employed while the basic test procedure described below was followed.

Samples were placed on an aluminum witness block 1/2-in. thick and 1 in. wide. A layer of 0.001 in. polyethylene insulation was placed over the sample; then a luctie cover containing six pin switch leads (0.8 in. apart in a channel milled to closely fit over the MDF) was taped over the sample. A ground lead was clipped to one end of the MDF, while a No. 6 blasting cap was taped to the other. This assembly was then placed inside a 1/4-in.-thick steel test chamber which was enclosed in a 1/2 in. thick lucite vented box (located in the hood as shown in Figure 7). Timing

TABLE 7

PROPERTIES OF MILD DETONATING FUZE

Sample	Material	Loading, Grains/ft	Explosive, wt%	Outer Diameter, in.	Total Weight, g/ft	Source
F	DIPAM	2.1	6.9	0.040	1.91	*PA
M	DATB	12.4	5.54	0.105	14.5	**LRL
T	NASA-1	5.7	3.23	0.091	11.4	NASA

*Picatinny Arsenal
**Lawrence Radiation Laboratory

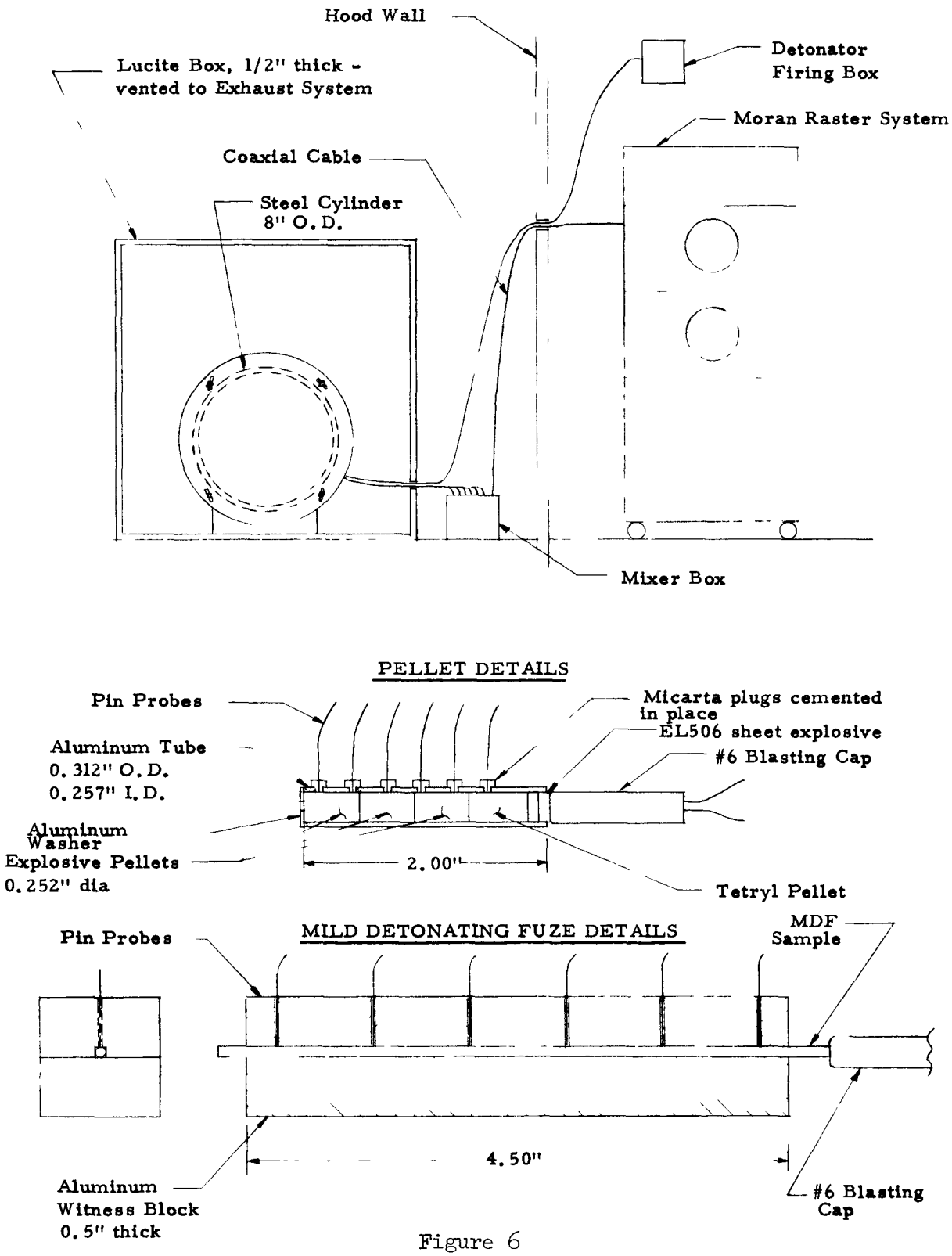

Figure 6

Detonation Velocity General Assembly

Figure 7

Detonation Velocity Confinement System

between pins was measured using a Moran 101A raster scope system accurate to within ±0.5%. Since pin locations were measured to ±0.1% accuracy, the variations in velocity observed vs those due to the explosive are believed to be a result of delays in pin closing caused by the layer of 0.001-in. polyethylene insulation placed between the MDF and pins. The test design is being modified to permit elimination of this insulation on future tests.

2. Pressed Explosive Velocity Test Method

In addition to the MDF velocity tests just described, tests were made on pressed pellets. Because of the size of the capsules, explosive samples were limited to 0.25 in. dia and 1.8 g total weight. Pellets of the pure explosives were pressed at 30,000 psi using the solvent pressing technique to attain high densities (84-97% MD). To minimize density variations, pellet length was limited to twice its diameter. Because of the weight limitation, three pellets of irradiated explosive and an unirradiated tetryl booster pellet of the same dimensions were used in each test. To assure high-order detonation, the pellets were confined in an aluminum tube (0.312 in. OD, 0.257 in. ID). This was sufficient to make AGH detonate high order in half of its unconfined failure diameter.

As an additional check on performance, a steel witness block was placed over the end of the explosive column. This assembly is shown in Figure 8. Samples were irradiated in the aluminum tube to ensure that the test could be made even if the pellets crumbled or swelled. Lead wires were glued in place and the tube taped into the firing assembly after irradiation. Because of the radioactivity of the tube, accurate assembly of the pins could not be checked. Some of the pins were slow to close - possibly due to a glue-filled gap between the end of the pins and the explosive. Premature closing may have been caused by jetting through air gaps between pellets or between pellets and the confining tube wall. In future tests, pellets will be irradiated and then loaded into pre-assembled tubes. Any gaps can therefore be filled with grease to prevent jetting.

3. Results

Results of these tests are summarized in Table 8, and are reported in detail in Table 9. Because sample size was limited, only a

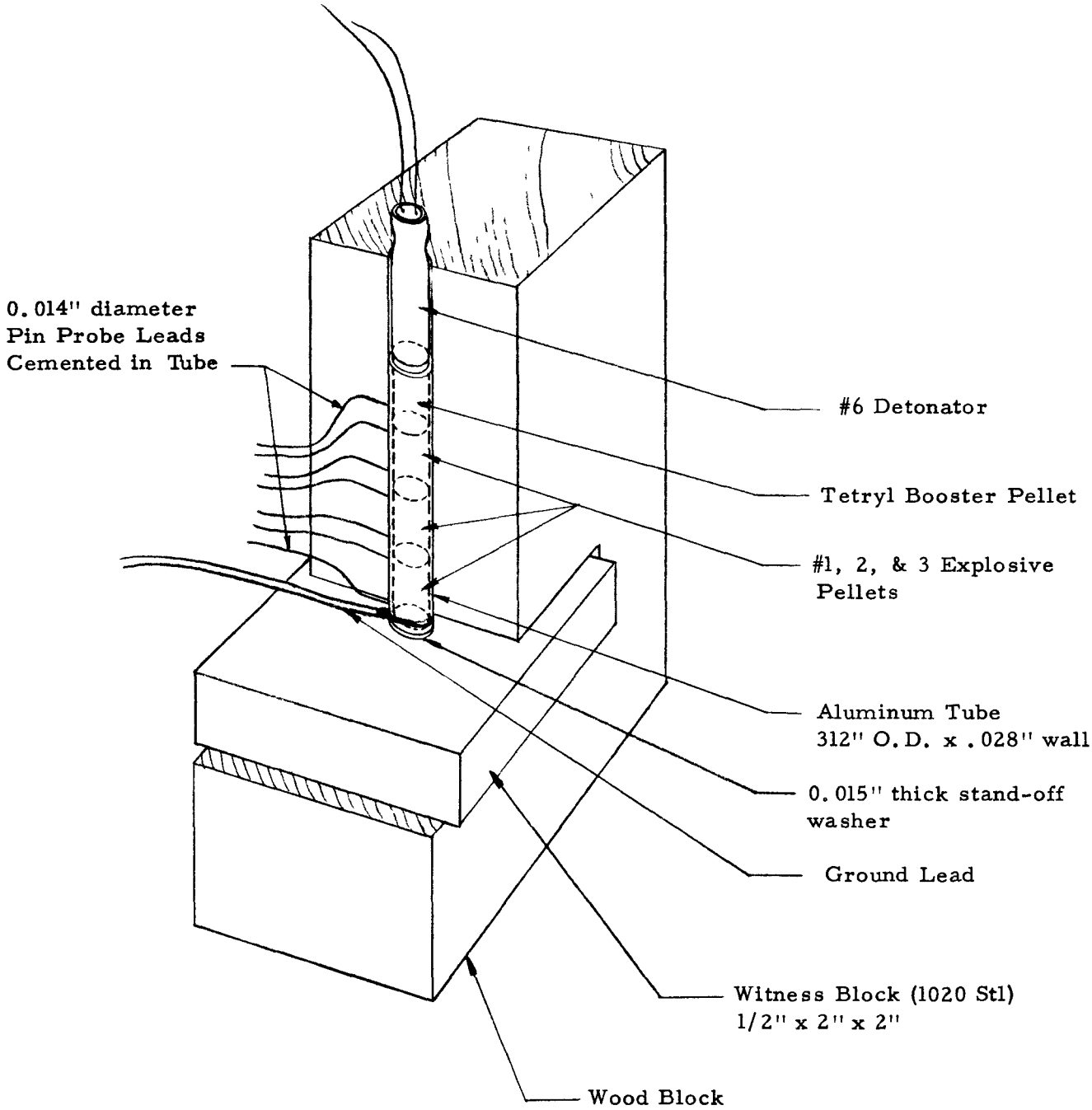

Note: Components will be taped in place; tape not shown for clarity.

Figure 8

Pressed Explosive Velocity Test Assembly

TABLE 8

AVERAGE DETONATION VELOCITIES

Material	Sample No.	Detonation Velocity and Density[1]							
		Observed				Corrected to 90% Crystal Density			
		AGC Std	36 min	120 min	180 min	NOL Std	AGC Std	120 min	180 min
NASA-1	A	7000 (1.625)		7150 (1.607)	6450 (1.604)	6940 (1.665)	7132 (1.665)	7341 (1.665)	6651 (1.665)
TATB	H	7700 (1.754)		6375 (1.546)	7150[2] (1.523)	7487 (1.742)	7666 (1.742)	6935 (1.742)	7775[2] (1.742)
NONA	J	7220 (1.666)	-	7170 (1.608)	6970[2] (1.503)		7022 1.60	7146 (1.60)	7251[2] (1.60)
DIPAM	O	7540 (1.690)		7330 (1.664)	6580 (1.572)	7300 (1.61)	7223 (1.61)	7118 (1.61)	6731 (1.61)
DIPAM	F	5980[3]	5545[3]	5160[3]	-	-	-	-	-
DATB	W	6850 (1.512)		6300 (1.527)	- -	7191 (1.651)	7247 (1.651)	6654 (1.651)	- -
DATB	M	5787[3]	5724[3]			6967[3][4]			
HNS	V	6806 (1.590)		6830 (1.520)	6730 (1.440)	-	6733 1.568	6989 (1.568)	7154 (1.568)

[1] First figure listed for each sample is velocity (m/sec); figure immediately below (in parenthesis) is the density (g/cu cm) at which velocity was observed.

[2] Irratic results due to excessive swelling and cracking of pellets.

[3] Density unknown.

[4] Data obtained from Lawrence Radiation Laboratory.

TABLE 9

DETONATION VELOCITY DATA

Material	Sample	Pin to Pin Velocity (m/sec) Pin 1-2	Pin 2-3	Pin 3-4	Pin 4-5	Velocities Included in Avg	Average Velocity (m/sec)	Approx Min in Reactor	Average Density (g/cu cm) - Last Two Pellets	Remarks
						Pressed Pellets				
NASA-1	A	6350	8700	5880	8140	2-5	7000	0	1.625	
NASA-1	A-3	8410	7030	5990	6450	2-5	6450	180	1.604	Pin 1 slow to close
NASA-1	A-4	6160	7560	6800	7140	2-5	7150	120	1.607	-
TATB	H	6630	7310	8280	7510	2-5	7700	0	1.754	-
TATB	H	7650	7650	7540	7560	1-5	7600		1.694	Pin 2 slow to close
TATB	H-3	6775	5990	9300	6920	2-5	7150	180	1.523	Pellets expanded excessively
TATB	H-4	16,300*	5150	6450	6300	3-5	6375	120	1.546	Pin 1 slow to close
NONA	J	8000	7110	7020	7525	2-5	7220	0	1.060	-
NONA	J-3	8600	6260	4770	6970	4-5	6970	180	1.503	Pellets (3-4) badly cracked and chipped
NONA	J-4	7230	7340	5840	9080	2-5	7170	120	1.608	Pellets (3-5) chipped
DIPAM	O	6975	7570	7300	7800	2-5	7540	0	1.090	-
DIPAM	O-3	6430	5970	8250	6200	2-5	6580	180	1.572	-
DIPAM	O-4	7720	7610	6890	7550	2-5	7330	120	1.064	-
HNS	V	7410	6700	5770	6100	2-5	6806	0	1.590	-
HNS	V-3	6350	7250	5810	6890	2-5	6730	180	1.440	-
HNS	V-4	6840	6840	6440	7200	1-5	6830	120	1.520	-
DATB	W	9290	5040	6370	10,850	2-5	6710	0	1.570	Large ρ variation
DATB	W	6210	6900	7260	6460	2-5	6850	0	1.512	-
DATB	W	6870	6500	7475	6515	2-5	6770	0	1.475	Low ρ
DATB	W-4	20,000*	9080	5850	5175	2-5	6300	120	1.527	Pin 1 and 2 slo to close
DATB	W-3	8730	6280	5980	7650	2-5	6560	180	1.465	-

Material	Sample	Pin to Pin Velocity (m/sec) Pin 1-2	Pin 2-3	Pin 3-4	Pin 4-5	Velocities Included in Avg	Average Velocity (m/sec)	Approx Min in Reactor	Overall Avg Velocity (m/sec)	Remarks
						Mild Detorating Fuzes				
DATB	M	5700	5850	6025	5950	1-5	5800	0		Bar 4
DATB	M	5750	5500	5360	6230	1-5	5700	0	5787	Bar 2
DATB	M	10,380*	5950	4180	9260	2-5	5810	0		Bar 6, average velocity from 3 to 5 was 5700
DATB	M-1	6950*	5760	6170	5580	2-5	5837	120		Bar 7
DATB	M-1	6325	6100	4970	5300	1-5	5610	120	5724	Bar 1
DATB	M-2	6490	5780	4970	6940	1-5	5960	180		Bar 11
DATB	M-2	5690	7390	5710	5640	1-5	6040	180	6000	Bar A
DIPAM	F	5950	5990	5910	-	1-4	5980	0	5980	Bar 12
DIPAM	F-1	5300	5290	5650	5400	1-5	5400	36		Bar 8
DIPAM	F-1	5790	5825	5600	5510	1-5	5690	36	5545	Bar 5
DIPAM	F-2	5200	5280	4940	4610	1-5	4990	120		Bar 9
DIPAM	F-2	5070	5180	4570	7180	1-5	5330	120	5100	Bar 10
NASA-1	T-0	5330	5890	4670	5720	1-5	5360	0		Bar 1A
NASA-1	T-0	5570	4790	6530	5010	1-5	5400	0	5380	Bar 2A
NASA-1	T-1	5970	4480	5490	4330	1-5	4970	120		Bar 3A
NASA-1	T-1	5810	4730	5090	4050	1-5	4840	120	4885	Bar 4A
NASA-1	T-2	4110	5970	4660	-**	1-4	4980	180		Bar 5A
NASA-1	T-2	3760	5040	2610	-**	1-4	3540	180	4260	Bar 6A

*Omitted (pin closed too slowly).
**Lower section of mild detonating fuze melted.

Table 9

rough measurement of velocity could be made. Accuracy is estimated to be within ±300 m/sec. Generally, velocities decreased with decreasing density as expected (Reference 7). After density loss is accounted for. no significant changes in velocity were observed. Less than 10% change in velocity occurred due to dilution of the explosive by less energetic (radiation-produced) decomposition products in all of the samples.

a. Mild Detonating Fuze (MDF)

Tests were made on irradiated samples of three explosives available in MDF form: AGM (DATB), AGF (DIPAM), and AGT (NASA-1). The velocity of DIPAM MDF decreased much more than the DIPAM pellets, probably due to its smaller diameter (0.040 in. OD) - thus making its velocity more sensitive to a decrease in density. If MDF is used in the NERVA Countermeasure system, its radiation stability must be accurately known in view of its sensitivity to changes (smaller diameter). Also, MDF should not be the only velocity test considered, since the density of the charge cannot be accurately determined, and the lead sheath's radioactivity prohibits immediate analysis.

b. Pressed Explosive Pellets

Comparative detonation velocity data of the explosive pellets are provided in Table 8. The NOL data on the DIPAM explosive was obtained from NOLTR 63-16, and is illustrated in Figure 9. As noted, deontation velocity varies with density and diameter. In addition, heavily confined charges detonate faster than lightly confined ones. Sufficient data is not available to permit calculating the exact effect of confinement and diameter. However,these factors are related by Jones (Reference 8) as indicated below.

$$\frac{D}{D_i} = 1 - \frac{a}{2R} \qquad \text{(no confinement)}$$

$$\frac{D}{D_i} = 1 - \frac{2.17 \left(\frac{a}{R}\right)^2}{W_C/W_e} \qquad \text{(light confinement - used in AGC tests)}$$

$$\frac{D}{D_i} = 1 - 0.88 \left(\frac{a}{R}\right) \sin \phi \qquad \text{(heavy confinement - used in NOL tests)}$$

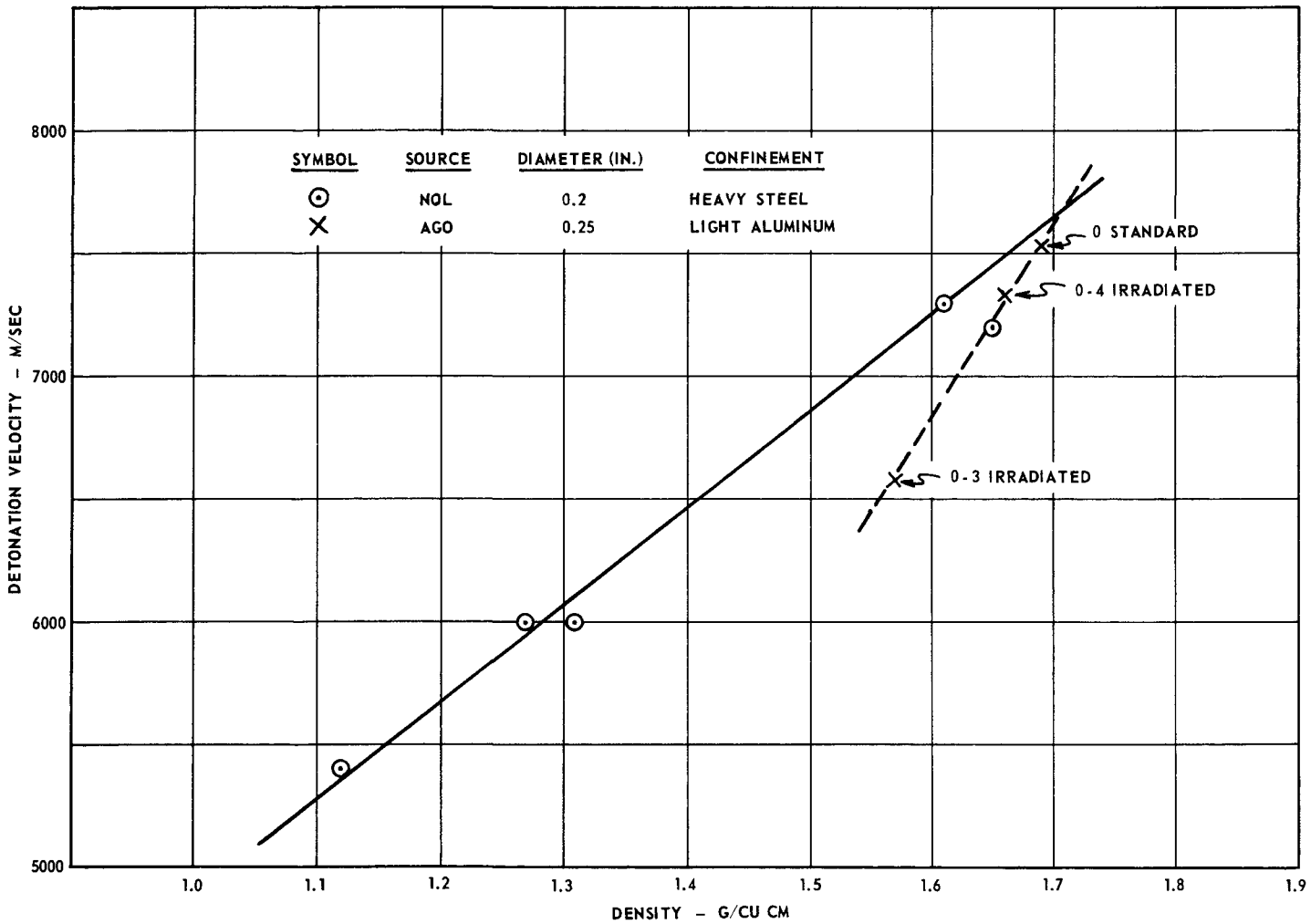

Figure 9

DIPAM Detonation Velocity vs Density

where

D = observed detonation velocity

D_i = ideal detonation velocity at infinite diameter

R = radius of charge

a = reaction zone length = $\frac{3}{4} \tau D$

τ = burning rate = $Ae^{\frac{-E}{RT}}$

$$\tan \phi = \frac{\rho_o}{\rho} \sqrt{\frac{D_o^2}{D^2} - 1}$$

W_C = weight of confining material per unit length

W_e = weight of explosive per unit length

Additional data is required to accurately evaluate the reaction zone length. Using the data reported in NOLTR63-16, the following values have been calculated for AGO:

$$\phi = 11^\circ 25', \text{ when } \rho = 1.60$$

$$a = 0.0675 \text{ cm}$$

$$D_i = 7500 \text{ m/sec}$$

The corrections due to changes in density can be determined within $\pm 10\%$ from NOL data reported in NOLTR 63-16, 63-265, 61-155, and the Third Detonation Symposium. The corrections used to correct the observed velocities to those at 90% TMD in Table 8 are provided in Table 10.

The results for velocity-density dependence over a limited range can be represented by a straight line of the form $D = A + B\rho$. For example, this correlation has been used to fit the NOL data on DIPAM as shown in Figure 9. The slope of the velocity-density line $\left(\frac{dD}{d\rho}\right)$ on this plot

TABLE 10

VARIATION IN DETONATION VELOCITY WITH DENSITY

Explosive	Sample	TMD	90% TMD	dD/dρ	Range of TMD After Irradiation, %
NASA-1	AGA	1.85	1.665	3330	84.5 - 88.7
TATB	AGH	1.938	1.742	2852	71.7 - 84.6
NONA	AGJ	1.78	1.60	~3000	82.6 - 92.2
DIPAM	AGO	1.79	1.61	3960	85.5 - 94.1
HNS	AGV	1.74	1.568	3314	82.4 - 89.6
DATB	AGW	1.837	1.651	2852	82.0 - 84.0

Table 10

is equal to B in the above equation. To correct velocities to 90% TMD (theoretical maximum density), it is only necessary to know this parameter, since the velocity-density equation takes the form

$$D_2 = B\ (\rho_2 - \rho_1) + D_1$$

where

D_2 = detonation velocity at 90% TMD, m/sec

ρ_2 = TMD, g/cu cm x 0.90

D_1 = observed detonation velocity, m/sec

ρ_1 = density of sample, g/cu cm

When dilution of the explosive occurs, such as that caused by radiolytic decomposition, the decrease in velocity is expected to be larger than the amount due to density alone. This appears to be true in the case of DIPAM as shown in Figure 9.

c. Plate Dent

Plate dent provides a relative indication ($\pm$10%) of explosive performance. High-order detonations were obtained from all samples tested, since no noticeable dent will be produced if the explosive merely deflagrates. The data obtained are listed on Pages 43 and 44 of Reference 1. Since weight loss was less than 10%, a significant decrease in performance would not be expected. Plate dent data show this to be the case, since no appreciable change in plate dents occurred. In the case of MDF, no large variations in output and only two failures occurred (in AGT-2), even though this form is more sensitive to loss of explosive than the larger pressed pellets.

. THERMAL STABILITY

Three tests of thermal stability were made, because no single test provides a complete understanding of the thermal behavior of pseudo stable materials. These tests were of vacuum stability, differential thermal analysis (DTA), and explosion temperature.

1. Vacuum Stability

Vacuum stability (References 9 and 10) provides a good long-term stability (2-hour) measurement on materials which evolve gas as they decompose. It is generally interpreted as a "go, no go" test at the specific temperature being investigated. Therefore, two materials may have different ultimate failure temperatures, but they will both pass vacuum stability at a lower temperature. Since vacuum stability is more stringent than the other tests, it is useful in establishing an unqualified safe upper temperature limit. (It should be noted that explosives can stand even higher temperatures for shorter times, as shown by the explosion temperature.) To be most useful, the vacuum stability test temperature should be high enough for the materials to pass, while being near failure.

Vacuum stability test results are summarized in Table 11. Since a temperature of 260°C was used by NOL to check the explosives before irradiation, our tests were also performed at this reading. After the first tests on irradiated samples failed at this temperature, a few tests were run at 200°C; the majority of samples were then run at 150°C.

The criterion (Reference 11) used to judge these results is shown at the bottom of Table 11. On this basis, NASA-1, black powder, AK-14, DIPAM, TATB, and DATB were the only materials which unquestionably passed the 150°C vacuum stability test after a 120 min irradiation. Since errors in vacuum stability are caused by leaking joints, this type of error is not uncommon. The results in Table 11 that are marked with an asterisk are believed to be high for this reason, since gas evolution is not expected to decrease after a longer irradiation time.

If these assumptions are correct, then NONA would also be expected to pass the 150°C vacuum stability test after a 2-hour irradiation. In addition, ANP 3095 propellant might have passed at 150°C, since it passed the test at 120°C. The TATB, NONA, DIPAM and HNS samples were irradiated for 3 hours and failed the subsequent vacuum stability test at 150°C.

TABLE 11

VACUUM STABILITY RESULTS

			Average Gas Volume (cu cm/g/hr)											
			260°C Test Temp			200°C Test Temp			150°C Test Temp				120°C Test Temp	
Code No.	Material	Test Duration (hr)	at 0 min Irrad Time	at ~36 min Irrad Time	at ~136 min Irrad Time	at 0 min Irrad Time	at ~136 min Irrad Time	at ~180 min Irrad Time	at 0 min Irrad Time	at ~36 min Irrad Time	at ~136 min Irrad Time	at ~180 min Irrad Time	at 0 min Irrad Time	at ~136 min Irrad Time
A-0	NASA-1	40	0.217	-	-	-	-	-	-	-	-	-	-	-
A-1	NASA-1	40	-	0.525	-	-	-	-	-	-	-	-	-	-
A-2	NASA-1	18.3	-	-	-	-	0.506	-	-	-	-	-	-	-
E-0	AK-14	40	-	-	-	0.008	-	-	< 0.008	-	-	-	-	-
E-1	AK-14	24, 2.7	-	Failed	-	-	-	-	-	3.917*	-	-	-	-
E-2	AK-14	2.33	-	-	-	-	-	-	-	-	0.018	-	-	-
H-0	TATB	40, 2.33	Failed	-	-	-	-	-	0.110	-	-	-	-	-
H-1	TATB	2.33	-	-	-	-	-	-	-	-	-	5.440	-	-
H-2	TATB	18.3	-	-	-	-	1.045	-	-	-	-	-	-	-
J-0	NONA	2.33	-	-	-	-	-	-	0.073	-	-	-	-	-
J-1	NONA	2, 2.33	-	-	-	-	-	Failed	-	-	-	6.460	-	-
J-2	NONA	0.5, 2.7	-	-	Failed	-	-	-	-	-	11.022*	-	-	-
L-0	NASA-2	2.33	-	-	-	-	-	-	0.258	-	-	-	-	-
L-2	NASA-2	2.33	-	-	-	-	-	-	-	-	1.921	-	-	-
L-3	NASA-2	2.33	-	-	-	-	-	-	-	4.022	-	-	-	-
O-0	DIPAM	40	Failed	-	-	0.021	-	-	-	-	-	-	-	-
O-1	DIPAM	2.33	-	-	-	-	-	-	-	-	5.172	-	-	-
O-2	DIPAM	0.5, 2.33	-	-	Failed	-	-	-	-	-	3.600	-	-	-
R-0	ANP-3095	2.33	-	-	-	-	-	-	-	-	-	-	0.154	-
R-2	ANP-3095	2.78	-	-	-	-	-	-	-	-	-	-	-	3.267
S-0	Black Powder		-	-	-	-	-	-	0.474	-	-	-	-	-
S-1	Black Powder	40, 2.7	-	Failed	-	-	-	-	-	3.748*	-	-	-	-
S-2	Black Powder	2.33	-	-	-	-	-	-	-	-	1.578	-	-	-
V-0	HNS	40	-	-	-	0.016	-	-	-	-	-	-	-	-
V-1	HNS	0.1, 2.33	-	-	-	-	-	Failed	-	-	-	13.27	-	-
V-2	HNS	0.5, 2.33	-	-	Failed	-	-	-	-	-	8.429	-	-	-
W-0	DATB	40	Failed	-	-	0.047	-	-	-	-	-	-	-	-
W-1	DATB	2.33	-	-	-	-	-	-	-	-	4.481	-	-	-

*Probably high results caused by a leaking joint

Stability Ratings:

Excessive = 5 + ml gas/g/hr
Moderate = 3-5 ml gas/g/hr
Slight = 2-3 ml gas/g/hr
Very Slight = 1-2 ml gas/g/hr
Negligible = 0-1 ml gas/g/hr

Table 11

2. Explosion Temperature

The explosion temperature test is basically a measure of relative thermal stability. This information is of particular importance in the NERVA system since high temperatures will be produced by gamma heating when the reactor is operating. The refinement of this technique developed by Zinn and Rogers (References 12 and 13) was used to increase the accuracy of the data. In the explosion temperature test the sample is pressed and confined in a No. 8 blasting cap, with dry asbestos being used in place of the cork to prevent steam explosions from giving erroneous results at high temperatures. These loaded caps are quickly immersed in a molten Wood's metal bath, and the time till explosion measured. This test was repeated at a number of different temperatures, and the results plotted in the form of log (t_{exp}) vs $\frac{1}{T}$. Using numerical solutions of the non-linear heat conduction equations developed by Zinn and Mader (Reference 7), it may be possible to use these results to predict the performance of the larger charges in the destruct system (See Appendix A). However, other parameters of thermal decomposition such as the activation energy (E), and thermal diffusivity (K) must be known before these calculations can be made.

The 5-sec explosion temperatures shown in Table 12 were obtained by interpolation of the explosion temperature data plotted in Figures 10 through 19.

The explosion temperature of black powder was decreased the least by irradiation because of its inorganic composition. The main charge explosives, in order of decreasing stability, were NASA-1, DATB, DIPAM, and TATB. NASA-1 was least affected because most of the products of decomposition are either gas or inert. The explosion temperature of materials that melt below their explosion temperature tends to be higher than would be expected, based on other thermal stability tests. This situation exists because temperature rise is decreased by the heat of fusion. The unusually high explosion temperature of DATB may be due to this effect.

The great change in DIPAM was in agreement with its high weight loss. The change in TATB, however, was unexpected in view of the

TABLE 12

EXPLOSION TEMPERATURE* SUMMARY

Material	Sample No.	Temp (°C) for Standard	Temp (°C) After 36 min Irradiation	% Change**	Temp (°C) After 120 min Irradiation	% Change**	Temp (°C) After 180 min Irradiation	% Change**
NASA-1	A	417	415	-0.5	374	-10.3	--	--
AK-14	E	406	313	-22.9	319	-21.4	--	--
TATB	H	392	--	--	287	-26.8	253	-35.5
NONA	J	440	--	--	360	-18.2	303	-31.1
NASA-2	L	375	247	-34.1	224	-40.3	--	--
DIPAM	O	371	--	--	287	-22.6	252	-32.0
ANP 3095	R	317	--	--	159	-49.8	--	--
Black Powder	S	324	337	+4.0	298	-8.0	--	--
HNS	V	382	--	--	314	-17.8	249	-34.8
DATB	W	403	--	--	344	-14.6	--	--

*Temperature at which sample explodes in 5 sec.

**From standard.

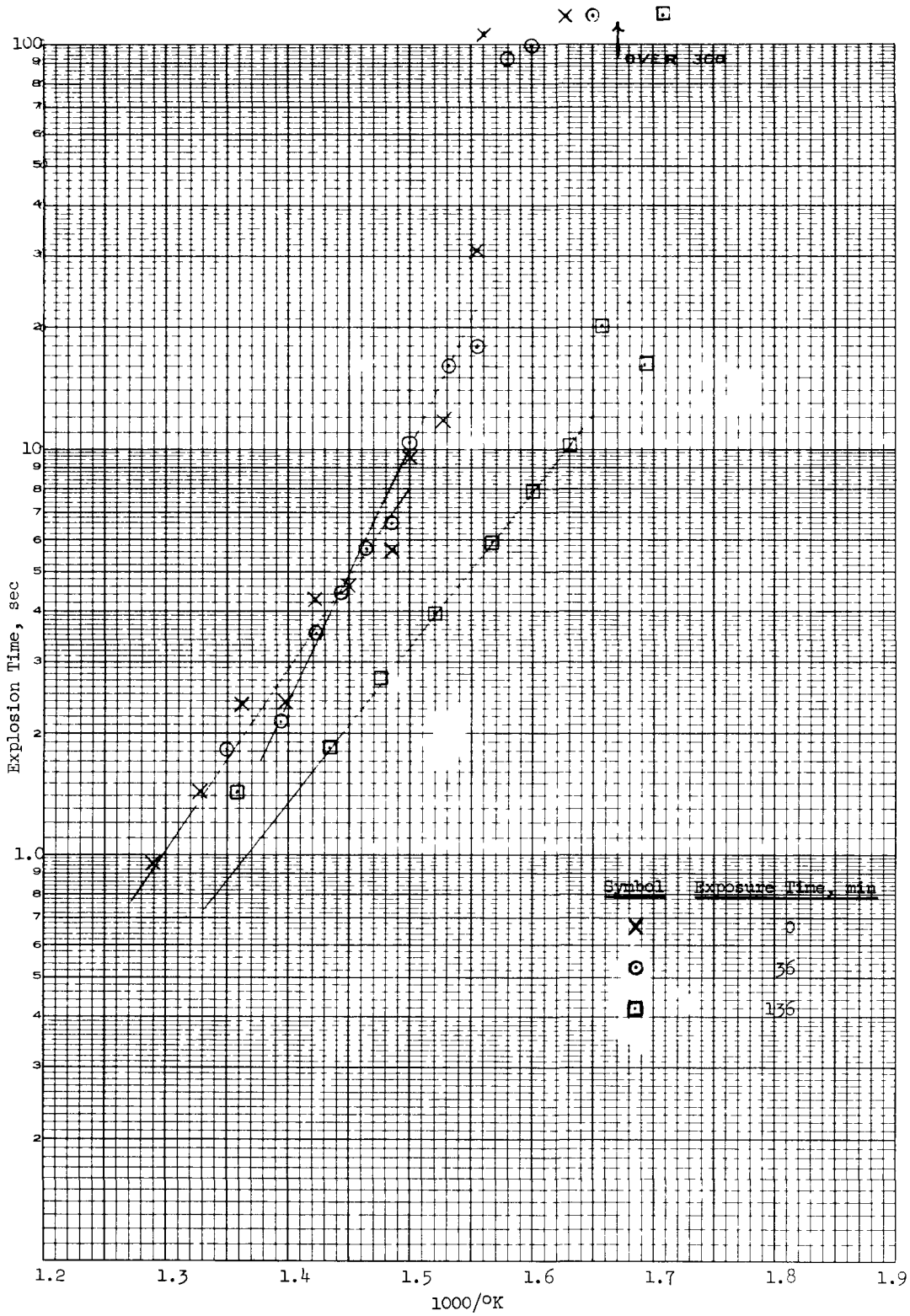

Figure 10

Explosive Temperature of NASA-1 Explosive

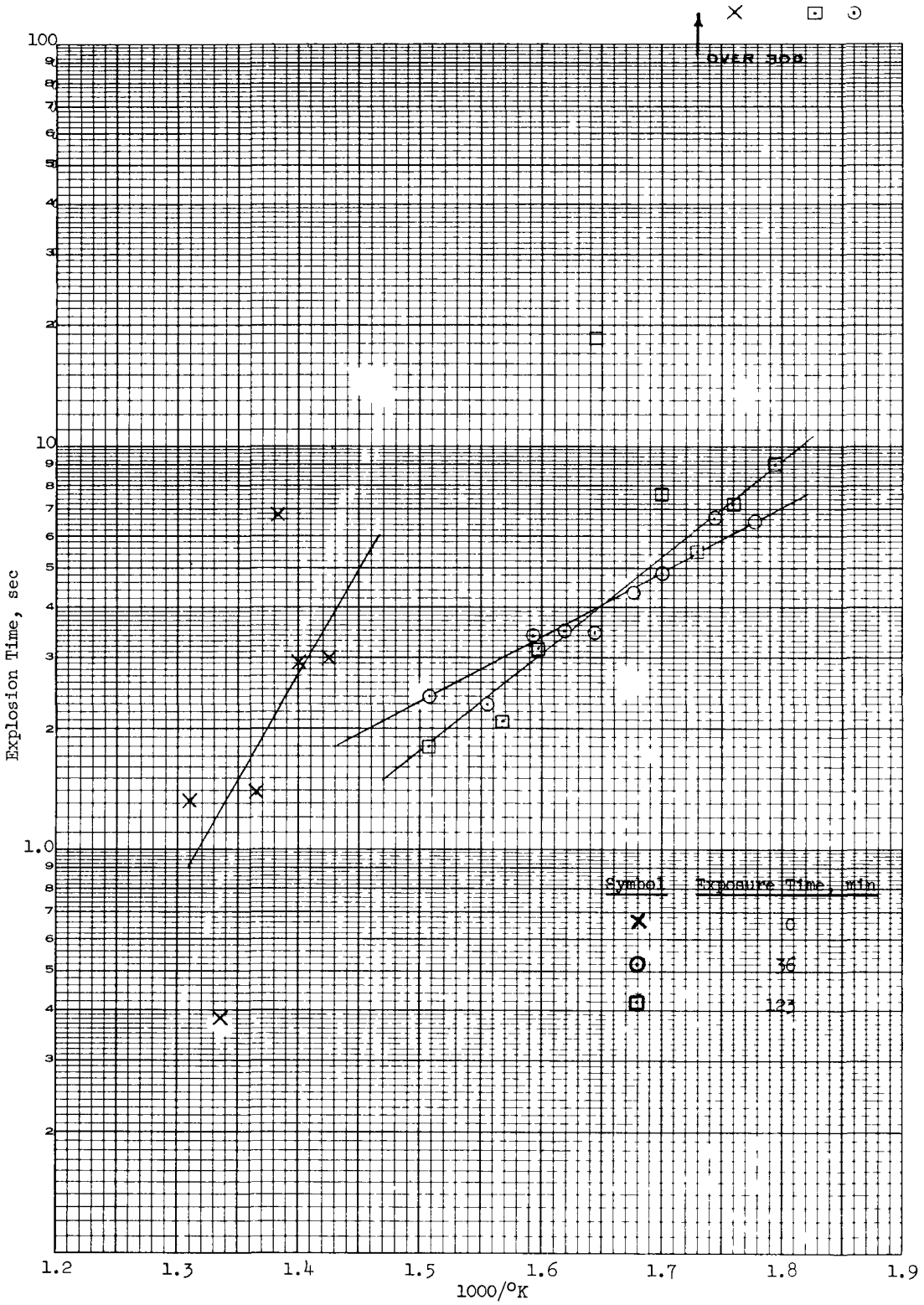

Figure 11

Explosive Temperature of AK-14 Propellant

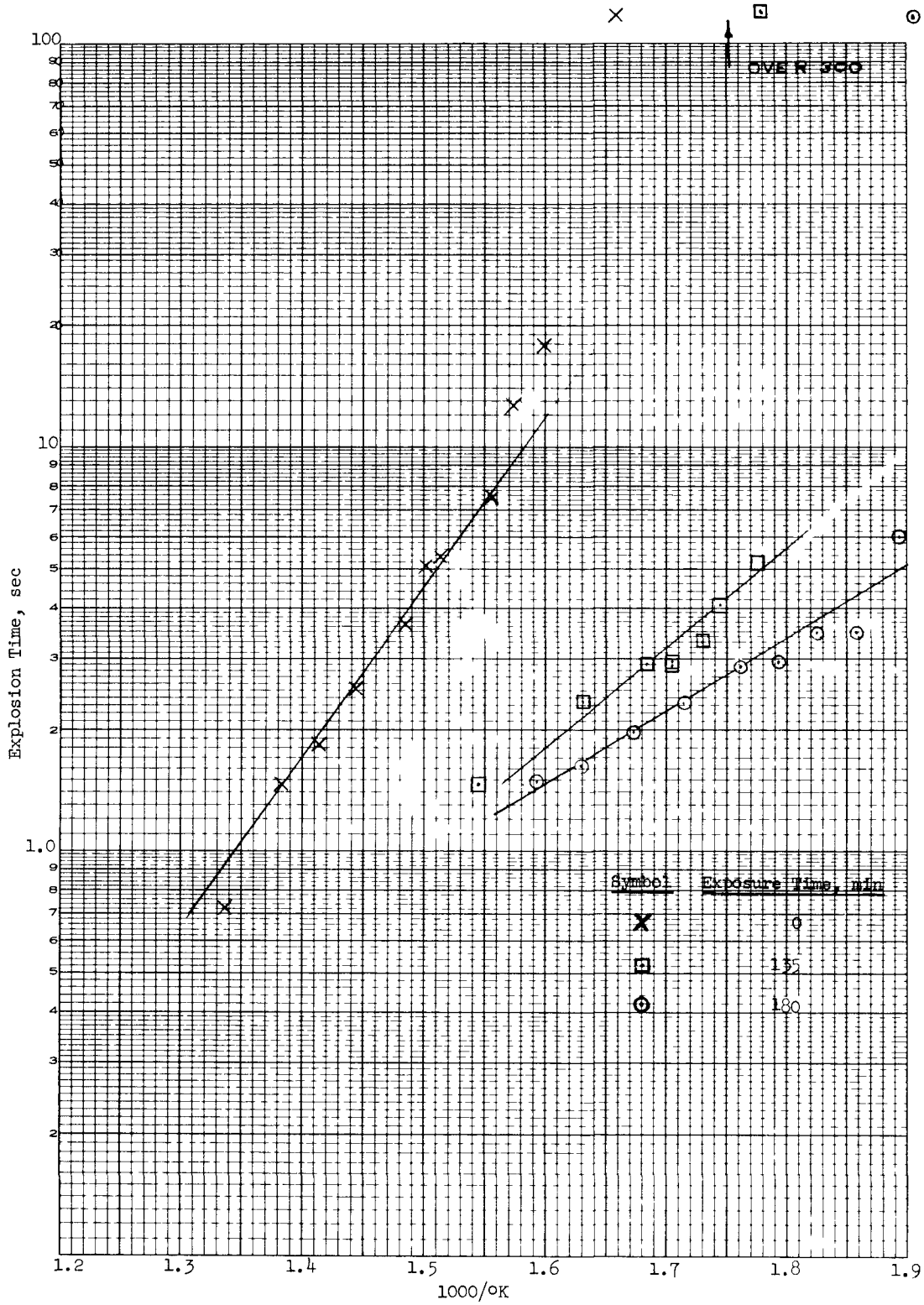

Figure 12

Explosive Temperature of TATB Explosive

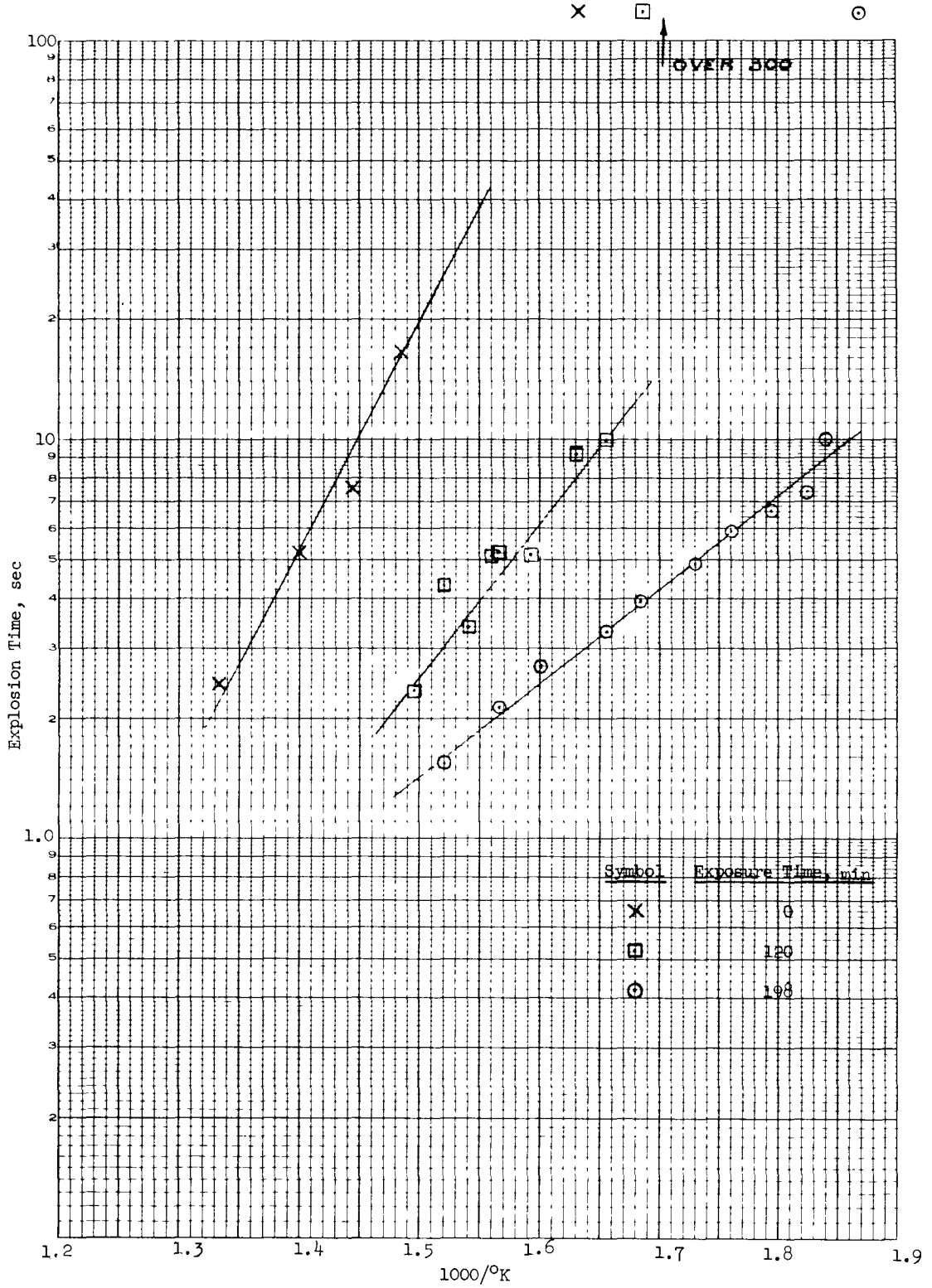

Figure 13

Explosive Temperature of NONA Explosive

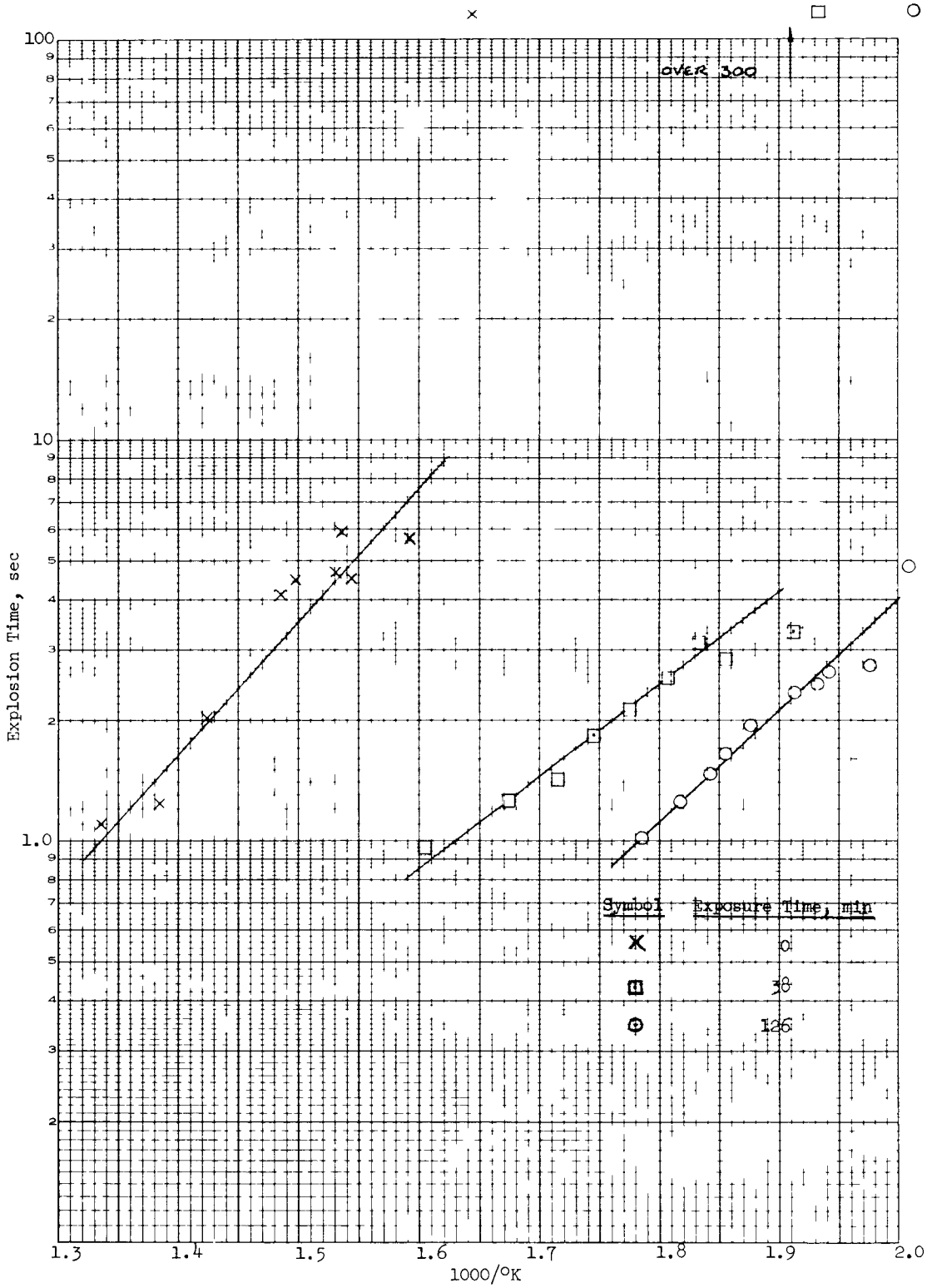

Figure 14

Explosive Temperature of NASA-2 Explosive

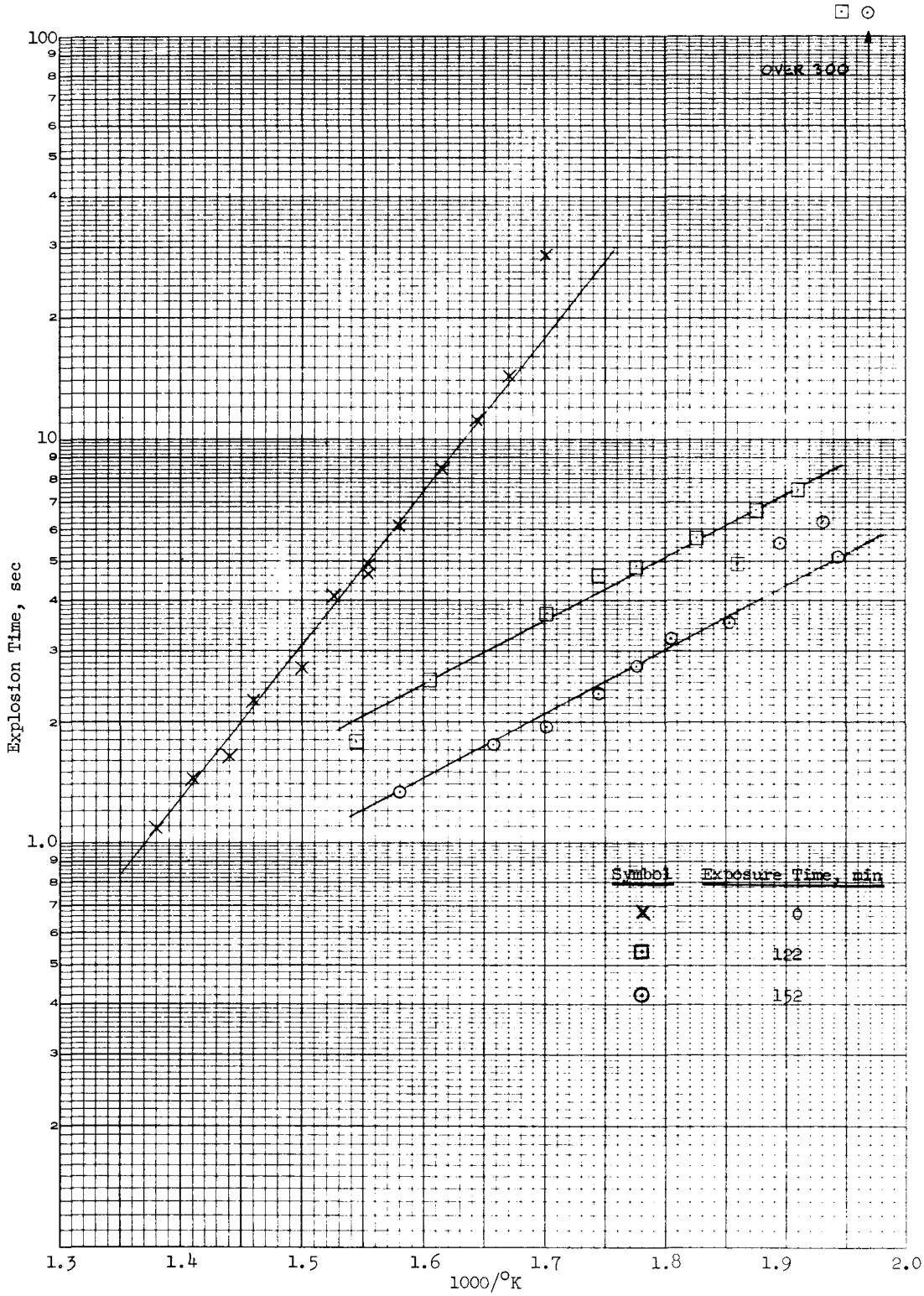

Figure 15

Explosive Temperature of DIPAM Explosive

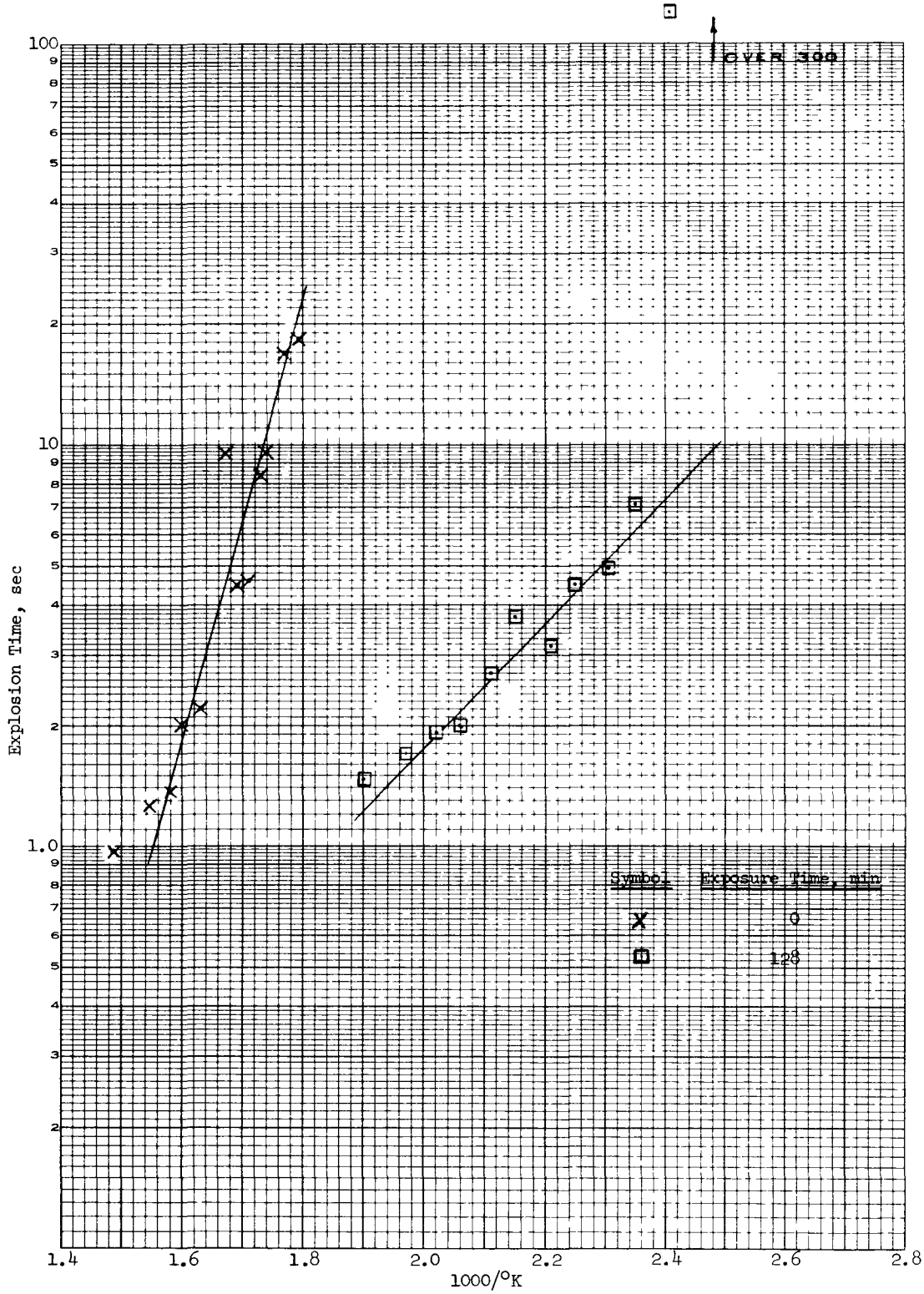

Figure 16

Explosive Temperature of ANP 3095 Propellant

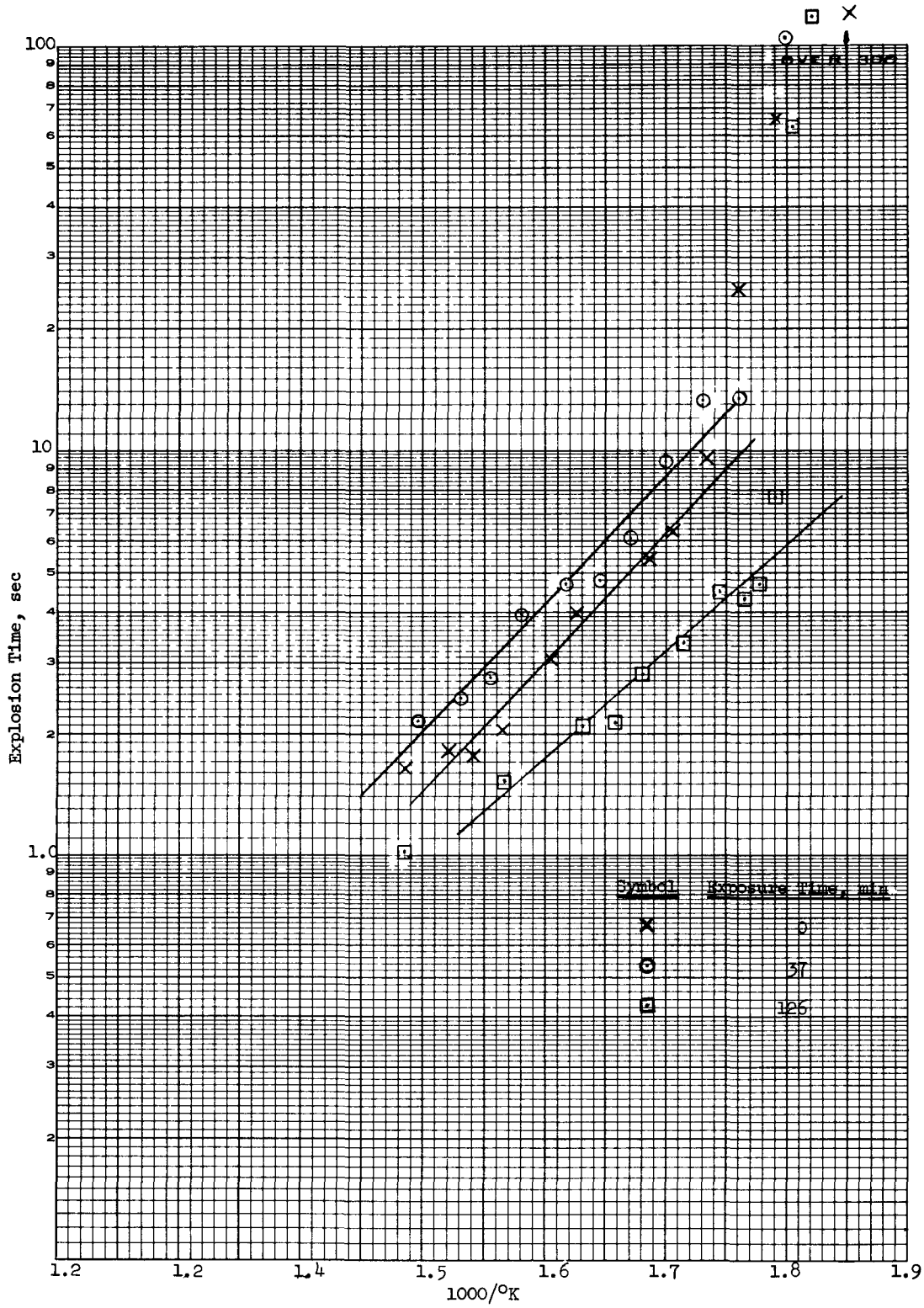

Figure 17

Explosive Temperature of Black Powder Initiator

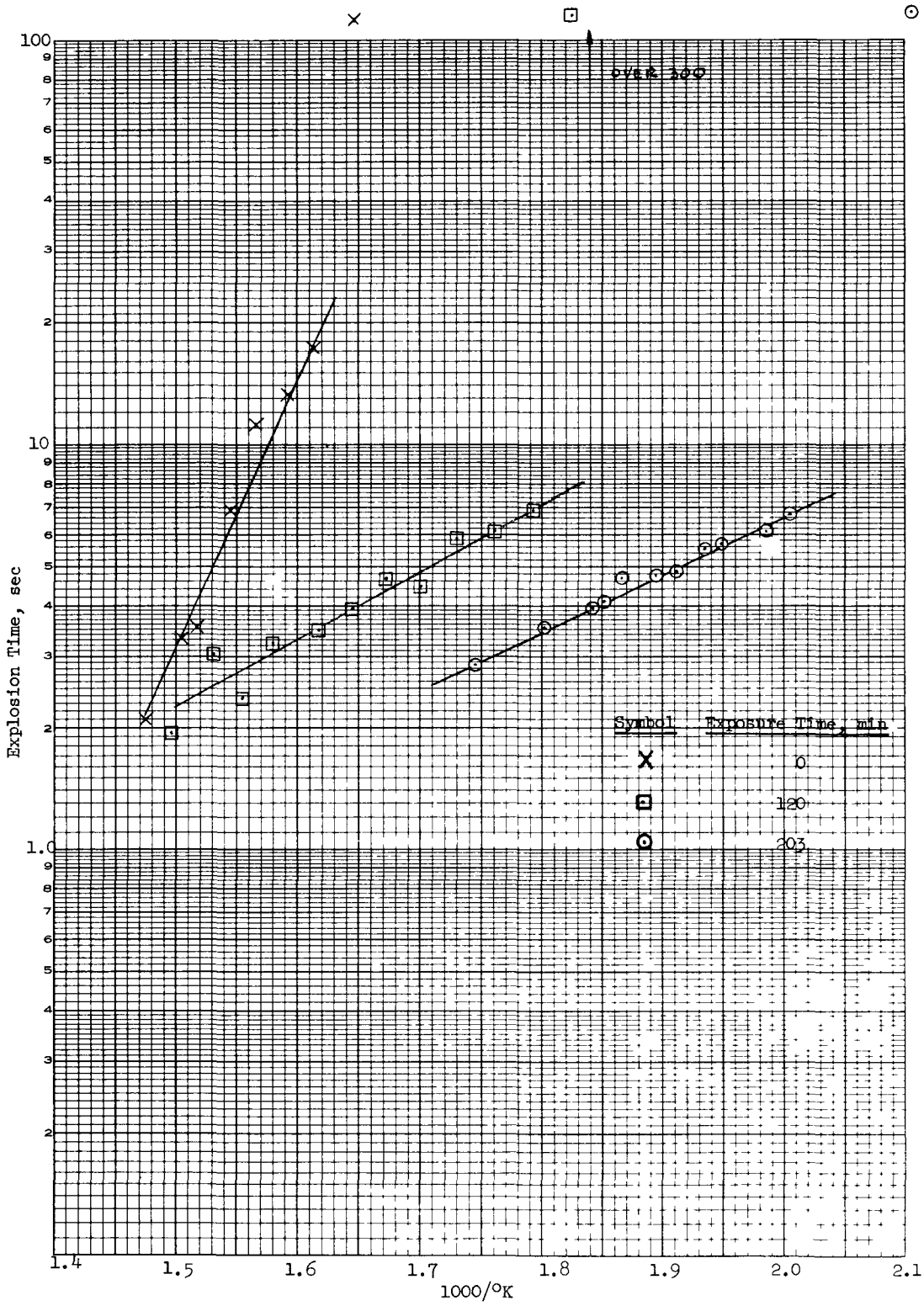

Figure 18

Explosive Temperature of HNS Explosive

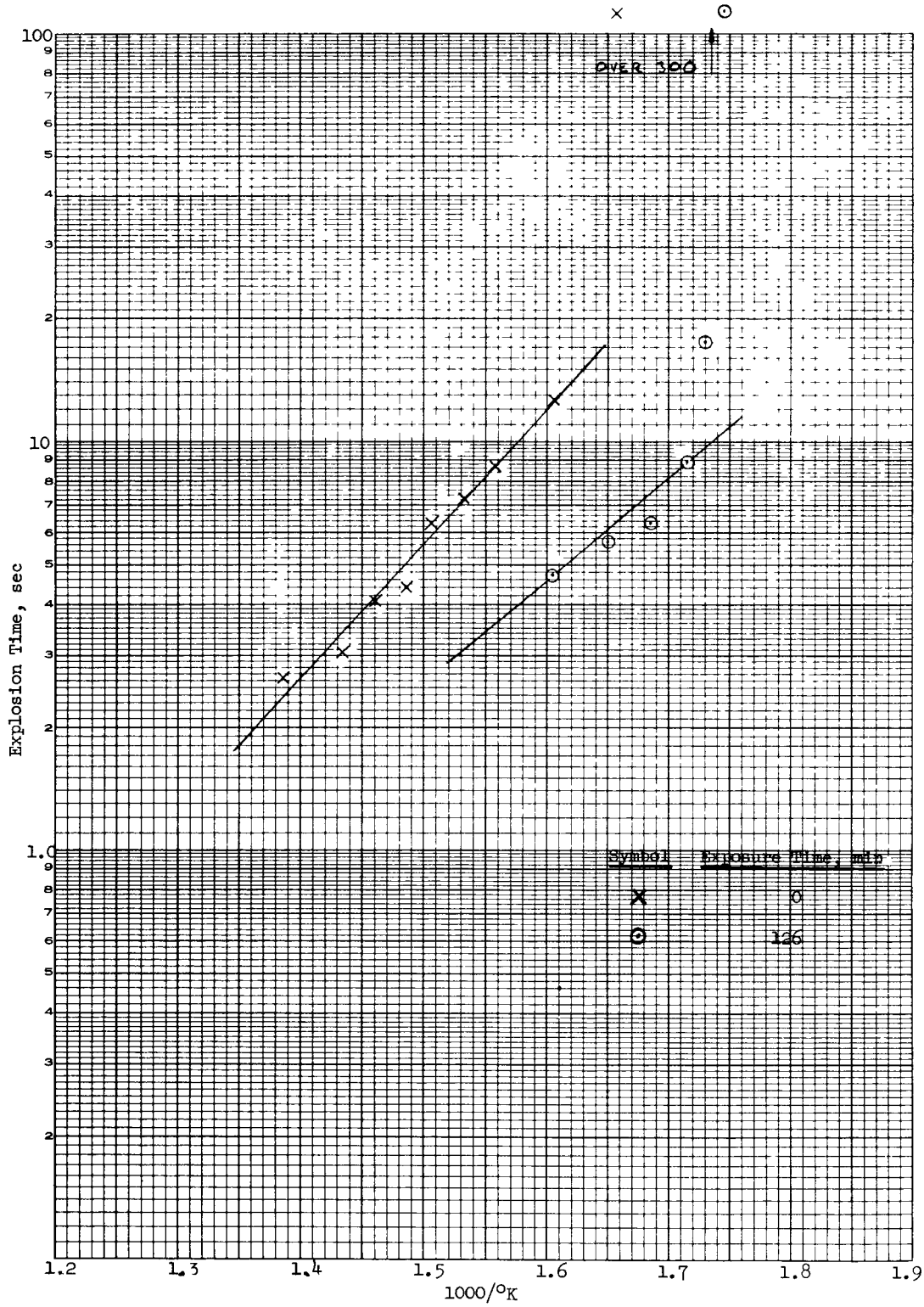

Figure 19

Explosive Temperature of DATB Explosive

small change in its weight loss and DTA exotherm. The decrease in explosion temperatures of the NONA booster explosive were about the same as that of HNS, but the temperatures were about 50°C higher. The decrease in explosion temperature of the NASA-2 primary explosive was in line with its high weight loss and general susceptibility to radiation damage.

The AK-14 propellant was similar to the explosives in its decrease of explosion temperature, but ANP 3095 had the largest decrease and the lowest explosion temperature of any of the materials tested. Before irradiation, this propellant passed a 6-hour storage test at 188°C (Reference 14); after irradiation it was found to explode in less than 5 sec at this temperature.

A few tests were duplicated after an elapsed time to check the effect of time on explosion temperature. In the case of TATB, sample AGH-2 fired in 2.90 sec at 311°C some 13 hours after irradiation, and in the same time after an elapsed time of 28 hours. On the other hand, the DATB sample (AGW-1) fired in 5.27 sec at 305°C after 23 hours, and in 17.55 sec at the same temperature after 39 hours. Sufficient data is not available at this time to draw any definite conclusions. However, it is assumed that little change in explosion temperature should occur in such a short time interval, and that the variations due to loading caused the variation in the AGW-1 sample. As can be seen from the data obtained, as the temperature decreases, the uncertainty or scatter of the data increases.

3. Differential Thermal Analysis

The DTA analysis exotherm peaks are provided in Table 13. Since the DTA procedure uses a continuous slow heating rate, rather than a sudden increase in temperature, the results are not directly comparable to the explosion temperature test. In most cases, the decrease in explosion temperature was larger than that in DTA exotherm temperature. This could be due either to the annealing effect of the slow temperature rise of the DTA - allowing crystal strains, ionization, and autocatalytic decomposition products to be removed before the exotherm temperature is reached - or to some of the explosion temperatures occurring on the first exotherm rather

TABLE 13

DIFFERENTIAL THERMAL ANALYSIS SUMMARY

Type	Material	Sample No.	DTA Exotherm Range, °C* (10° C/min Heating Rate) at ~0 min Expos Time	at ~36 min Expos Time	at ~120 min Expos Time	at ~180 min Expos Time	Remarks
Main Charge Explosive	NASA-1	AGA	375-387	363-383	340-385	-	
Main Charge Explosive	TATB	AGH	335-365	-	290-320	290-348	
Main Charge Explosive	DIPAM	AGO	311-318	-	290-304	260-288	Two Exotherms
Main Charge Explosive	DIPAM	AGO	297-308	-	255-265	257	
Main Charge Explosive	DATB	AGW	318-330	-	300-333	-	
Main Charge Explosive	DATB	AGW	302-317	-	-	-	Triple exotherms in standard sample
Main Charge Explosive	DATB	AGW	271-300	-	-	-	
Booster Explosives	NONA	AGJ	360-388	-	290-365	275-350	
Booster Explosives	HNS	AGV	333-338	-	298-323	290-323	
Booster Explosives	HNS	AGV	330-332	-	-	-	Triple exotherm in standard sample
Booster Explosives	HNS	AGV	307-329	-	-	-	
Primary Explosive	NASA-2	AGL	368	325-353	265-307	-	
Initiator	Black Powder	AGS	350-403	350-397	350-400	-	
Initiator	Black Powder	AGS	285-325	285-318	290-322	-	Double Exotherm
Propellants	AK-14	AGE	415-472	435-477	390-455		(345-373) Exotherm in standar disappeared after irradiation.
Propellants	ANP3095	AGR	265-320	-	300-317	-	Double exotherm (230-243 exotherm
Propellants	ANP3095	AGR	230-243	-	170	-	disappeared after irradiation)

*First temperature is start of exotherm, second temperature is peak.

Table 13

than the second. For example, with the ANP 3095 propellant, the explosion temperature dropped from 322 to 163°C after irradiation. Although the highest DTA exotherm remained the same, the DTA analysis showed a dramatic change in form. A new exotherm beginning at 170°C appeared which probably was responsible for the lower explosion temperature. In addition, the exotherm disappeared that had followed the NH_4ClO_4 melting point at 233°C.

REFERENCES

1. J. F. Jaklevick, Countermeasures Radiation Effects Program Phase I-B Data Summary and Final Report, GETC-1011, 1 March 1965 (Conf).

2. J. Kennedy, E. Bergmann, and R. Stresan, Initiation of Insensitive Explosives, ATL-TDR-64-44, AD 355490, October 1964.

3. Radiation Effects Methods and Data, AF Contract 33(600)-32054, NARF-58-43T, FZK-9-134, 7 Oct 1958.

4. H. Rosenwasser, Effects of Gamma Radiation on Explosives, ORNL 1720, Dec 1955.

5. M. Cook, Science of High Explosives, Rheinhold, 1958, p. 176.

6. J. Kaufman, "The Effect of Nuclear Radiation on Explosives," Proc Royal Soc of London, 246 (1254) - Series A, 29 July 1958, pp. 219-225.

7. J. Zinn and C. L. Mader, "Thermal Initiation of Explosives," J. Appl. Phys., 31, No. 2, p. 323-328, Feb (1960).

8. H. Eyring et al., "Stability of Detonation," Chem Rev., p. 69-181 (1949).

9. A. J. Clear, Standard Laboratory Procedures for Sensitivity, Brisance, and Stability of Explosives, FRL-TR-25, Jan 1961.

10. A. H. Rosen and H. I. Simmons, Improved Apparatus and Techniques for Measurement of Vacuum Stability of Explosives at Elevated Temperatures, NAVORD 6629, 12 March 1959.

11. Explosive Compatibility, PATR 1783, 1950.

12. R. N. Rogers, "Thermal Initiation of Explosives," Ind & Eng Chem, Prod Res, & Dev., 1, 169 (1962).

13. J. Zinn and R. Rogers, "Thermal Initiation of Explosives," J Phys Chem, 66, p. 2646-2653 (1962).

14. First Summary Report of the Development of Solid Composite Propellants for High Temperature Operations, Aerojet Report R D110-01-SRI, July 1957-1958 (Conf).

ACKNOWLEDGMENT

The principal contributors to the analysis of Phase I-B of this program were Mr. W. E. Voreck, Head of the NERVA Section, and Mr. E. I. Lindberg, Test Engineer, Aerojet-General Corporation, Ordnance Research Division, Downey, Calif.

APPENDIX A

CRITICAL TEMPERATURE DETERMINATION

Using the methods described by Zinn, Mader, and Rogers (References 7, 12, 13 of basic text), thermal time constant and critical temperature have been derived as shown below.

I. THERMAL TIME CONSTANT

Thermal time constant = $\tau = \frac{a^2}{K}$

where

K = thermal diffusivity, $cm^2/sec = \frac{\lambda}{\rho C}$ (approximately 0.00066 $cm^2 sec$ for explosives)

a = radius (half the thickness of a slab)

ρ = density

λ = thermal conductivity

C = specific heat

In the explosion temperature test, a 0.040 g sample is pressed into a disk 0.0754-cm thick and 0.65-cm in dia confined between the bottom of the copper cup and the copper blast check disk. For this case, a - 0.0377 cm, and τ = 2.16 sec.

II. CRITICAL TEMPERATURE

Critical temperature (T_m) is the temperature below which the explosive reaches a stable steady state, and above which a runaway exothermic reaction occurs.

Zinn and Mader found that induction times (t_{exp}) conformed to the relationship

$$\frac{t_{exp}}{\tau} = \text{function}\left(\frac{E}{T_m} - \frac{E}{T_1}\right)$$

When $\frac{t}{\tau} = 1$, $\left(\frac{E}{T_m} - \frac{E}{T_1}\right) = 7.11$ (for slabs from Figure 3 of Reference 7).

From the explosion temperature plot of t_{exp} vs T_1, the value of T_1 can be determined for $t_{exp} = 2.16$ sec. Using this and the activation energy (E), the critical temperature (T_m) can be calculated for the explosion test geometry since

$$T_m = \frac{1}{\left(\frac{1}{T_1} + \frac{7.11}{E}\right)}$$

Conversion to a different geometry (the destruct system projectile) can be made by the following relationship:

$$\frac{1}{T_{m(2)}} = \frac{1}{T_{m(1)}} + \frac{R}{E}\left[\ln \frac{a^2_{(2)}\,\delta_{(1)}}{a^2_{(1)}\,\delta_{(2)}} + 2 \ln \frac{T_{m(1)}}{T_{m(2)}}\right]$$

where

δ is a dimensionless parameter

(3.32 for spheres, 2.00 for cylinders, and 0.88 for slabs)

APPENDIX B

PROPERTIES OF AK-14 MOD I PROPELLANT

Propellant AK-14 Mod I is a cast, fuel-oxidizer material produced by the Aerojet-General Corporation for aircraft and booster rocket use. It has the following composition:

Constituent	Wt% (nominal)
Potassium perchlorate	74.00
P-10 resin	24.75
Cumene hydroperoxide	0.25
P-33 carbon black	1.00
Cobalt octoate	As required for proper gel time

Other properties of this propellant are:

$Q = 967$ cal/g (expt)

$C_p = 0.248$ cal/g/$^{\circ}$C

$\gamma = 1.164$ at 1000 psi (calculation)

$T_p = 1950^{\circ}$K (calculation)

$n_b = 0.0324$ moles/g (calculation)

Vessel used for test: 2.25 in. Aeroscar, 1 KS-2800, 0.24 KS-9900, 2.2 KS-11,000, 2.2 KS-33,000 rockets.

Charge configuration: Usually tubular, internal-external burning.

Strand burner results are presented below.

Pressure (psi)	Rate (r) in./sec	Pressure Exponent (n)	Pressure Interval (psi)	Temperature °C
300	0.30	0.741	300-3000	15.5
600	0.50			15.5
900	0.68			15.5
1000	0.72			15.5
2000	1.22			15.5
3000	1.62			15.5

where

r is from oscillograph record and web thickness

n = slope of line drawn through data of log r vs log p

Other properties are as follows:

π_K = 0.36%/°C at K = 200 for P = 1775 psi at 10 (average) °C

σ_P = 0.09%/°C at P = 1000 for r_{av} = 0.738 in./sec at 10 (average) °C

C_D = 0.00889 lbm/lbf-sec at 1000 psi and 15.5°C (experimental)

I_{sp} = 177 lbf-sec/lbm at 1000 psi, and expansion ratio of 5.3 (expt)

ρ = 1.89 b/cm^3 = 0.068 lb/in.^{3}

Non-hygroscopic

Rupture produced by a stress of 1736 psi at 0.050 (loading rate) in./min/in. at 28.3°C

Tensile strength at -40°F is 1799 psi; at 60°F it is 1301 psi, and at +140°F it is 352 psi.

Composition of gas discharge (mol%) - H_2 = 18.00, H_2O = 13.70, CO = 44.65, CO_2 = 7.25, KCl = 16.40. Exhaust is smoky.

Service accepted. Plant capacity in existence is 75,000 lb/day. Ingredients are mixed and cast cold. Grains are then cured.

This propellant has performed consistently in Aerohvar, Aeroscar, and 2.2-KS-11,000, 2.5-KS-18,000, and other booster rockets.

For further information, see Picatinny Arsenal Report Serial No. 1676, Aerojet Engineering Report 462, and SPIA/M2e (Unit 352) March 1953.